

A novel regulatory mechanism network mediated by lncRNA *TUG1* that induces the impairment of spiral artery remodeling in preeclampsia

Yetao Xu,^{1,6} Dan Wu,^{2,6} Bingqing Hui,^{3,6} Lijun Shu,¹ Xiaotong Tang,¹ Cong Wang,¹ Jiaheng Xie,⁴ Yin Yin,¹ Matthew Sagnelli,⁵ Nana Yang,¹ Ziyang Jiang,¹ Yuanyuan Zhang,¹ and Lizhou Sun¹

¹Department of Obstetrics and Gynecology, First Affiliated Hospital of Nanjing Medical University, Nanjing 210029, Jiangsu Province, P.R. China; ²Department of Obstetrics and Gynecology, Women's Hospital of Nanjing Medical University, Nanjing Maternity and Child Health Care Hospital, 123 Tianfeixiang, Mochou Road, Qinhuai District, Nanjing 210004, China; ³Department of Oncology, First Affiliated Hospital of Nanjing Medical University, Nanjing 210029, Jiangsu Province, P.R. China; ⁴Department of Burn and Plastic Surgery, First Affiliated Hospital of Nanjing Medical University, Nanjing 210029, Jiangsu, China; ⁵University of Connecticut School of Medicine, Farmington, CT 06030, USA

Preeclampsia (PE) is associated with maternal and fetal perinatal morbidity and mortality, which brings tremendous suffering and imposes an economic burden worldwide. The failure of uterine spiral artery remodeling may be related to the abnormal function of trophoblasts and lead to the occurrence and progression of PE. Aberrant expression of long non-coding RNAs (lncRNAs) is involved in the failure of uterine spiral artery remodeling. However, the regulation of lncRNA expression in PE is poorly characterized. Here, we reported that hypoxia-induced microRNA (miR)-218 inhibited the expression of lncRNA *TUG1* by targeting FOXP1. Further RNA sequencing and mechanism analysis revealed that silencing of *TUG1* increased the expression of DNA demethylase TET3 and proliferation-related DUSP family, including DUSP2, DUSP4, and DUSP5, via binding to SUV39H1 in the nucleus. Moreover, *TUG1* modulated the DUSP family *in vitro* through a TET3-mediated epigenetic mechanism. Taken together, our results unmask a new regulatory network mediated by *TUG1* as an essential determinant of the pathogenesis of PE, which regulates cell growth and possibly the occurrence and development of other diseases.

INTRODUCTION

Preeclampsia (PE) is a pregnancy-specific disorder that originates from the placenta, characterized by new onset of hypertension after 20 weeks of pregnancy.¹ It occurs in approximately 5% of pregnant and lying-in women, leading to about 60,000 maternal and fetal deaths worldwide per year.^{2,3} The only way to cure PE is to induce delivery. Other clinical or experimental strategies are not effective for the treatment of patients with PE.⁴ The pathologic mechanism of PE (also known as placental dysfunction-mediated syndrome) has not been fully elucidated. The identification of new biomarkers for the prediction, diagnosis, and treatment of PE may improve maternal and infant outcomes.

In the first trimester of pregnancy, extravillous trophoblasts (EVTs) invade maternal decidua, causing spiral artery remodeling (SAR)

into highly dilated, low-resistance vessels. SAR ensures high blood flow to the uteroplacental bed.⁵ However, the function of EVT in patients with PE is impaired, resulting in arterial stenosis and an increased number of reactive vessels.⁶ Defective SAR contributes to the development of placental diseases, including hypoxia⁷ and/or imbalanced placental angiogenesis.⁸ These pathological changes lead to endothelial dysfunction and the occurrence of PE.^{9,10} Moreover, aberrant expression of placental genes has been shown to cause trophoblast dysfunction.¹¹ The regulatory roles of these genes in PE remain to be elucidated.

Previous studies of PE focused mainly on the dysregulation of protein-coding genes, which may be used as targets for clinical diagnosis and treatment. However, protein-coding sequences account for less than 2% of the human genome.¹² Long non-coding RNAs (lncRNAs) are a group of non-coding RNA transcripts that are more than 200 kb in length. Technological advances enable the investigation of lncRNAs in various human diseases.^{13,14} lncRNAs are implicated in a variety of physiological and pathological processes,¹⁵ such as cell metabolism,¹⁶

Received 3 August 2021; accepted 6 January 2022;
<https://doi.org/10.1016/j.ymthe.2022.01.043>.

⁶These authors contributed equally

Correspondence: Lizhou Sun, Department of Obstetrics and Gynecology, First Affiliated Hospital of Nanjing Medical University, Nanjing 210029, Jiangsu Province, P.R. China

E-mail: sunlizhou@njmu.edu.cn

Correspondence: Yuanyuan Zhang, Department of Obstetrics and Gynecology, First Affiliated Hospital of Nanjing Medical University, Nanjing 210029, Jiangsu Province, P.R. China

E-mail: zhangyuanyuan5518@jssph.org.cn

Correspondence: Ziyang Jiang, Department of Obstetrics and Gynecology, First Affiliated Hospital of Nanjing Medical University, Nanjing 210029, Jiangsu Province, P.R. China

E-mail: zyjiangchm@163.com

Correspondence: Nana Yang, Department of Obstetrics and Gynecology, First Affiliated Hospital of Nanjing Medical University, Nanjing 210029, Jiangsu Province, P.R. China

E-mail: nanayang210@163.com

disease-related development,^{17,18} cell growth,¹⁹ and others. In addition, aberrant lncRNA expression has been reported to positively or negatively regulate the genes related to different human diseases, including PE. Many studies have shown that lncRNAs regulate downstream genes via different mechanisms, including transcriptional, post-transcriptional, and chromatin modifications.²⁰ For instance, lncRNA *HOXA11-AS* is implicated in the transcriptional process of *RND3* by recruiting polycomb repressive complex 2 and lysine-specific histone demethylase 1 and in the post-transcriptional process of *HOXA7* by competing for microRNA (miR)-15b-5p, which inhibit trophoblast proliferation and migration in PE.²¹

lncRNA *TUG1* plays an important role in embryonic development and tumorigenesis.²² *TUG1* encodes a 7.6-kb-long polyadenylated lncRNA, which is distributed mainly in the nucleus. Abnormal expression of *TUG1* has been reported in various diseases, including PE.^{23,24} Our previous study showed that *TUG1* was downregulated in the placental tissues of PE patients compared with a control group. Also, *in vitro* experiments demonstrated that *TUG1* bound to the enhancer of *zeste 2* polycomb repressive complex 2 subunit, which recruited H3K27 to inhibit the transcription of *RND3*, thereby inhibiting trophoblast growth and migration in PE.²⁵ We planned to explore the underlying regulatory mechanism of *TUG1* in the pathogenesis of PE.

In this study, we found that hypoxia-induced miR-218 inhibited the expression of *FOXP1* at the post-transcriptional level and then inhibited the expression of *TUG1*. High-throughput sequencing analysis revealed that silencing of *TUG1* upregulated the expression of DNA demethylase *TET3* and the *DUSP* family, including *DUSP2*, *DUSP4*, and *DUSP5*, via binding to suppressor of variegation 39 homolog 1 (*SUV39H1*) in the nucleus. In addition, *TUG1* modulated the *DUSP* family *in vitro* through a *TET3*-dependent epigenetic mechanism. Taken together, we proposed a new *TUG1*-related pathway that regulated cell growth and migration in PE and may also be involved in the occurrence and progression of other diseases.

RESULTS

TUG1* epigenetically regulates the expression of *TET3* and the *DUSP* family by recruiting *SUV39H1

In a previous study we determined that *TUG1* can affect trophoblasts' biological function, including cell growth, migration, and network *in vitro*, further promoting the progression of preeclampsia.²⁵ *TUG1* can modulate trophoblast function by regulating the expression of multiple genes. To investigate the role of the *TUG1*-associated pathway in PE, we performed RNA sequencing analysis and generated gene expression profiles of HTR-8/SVneo cells transfected with siCon or small interfering RNA (siRNA) against *TUG1* (Figure 1A). The most differentially expressed genes were DNA demethylase *TET3* and proliferation-related *DUSP* family members, such as *DUSP2*, *DUSP4*, and *DUSP5* (Tables S6 and S7). Wu et al.²⁶ demonstrated that *TET3* plays a critical role in epigenetic reprogramming of human embryo, and *TET3* deficiency in the villus of human embryo might be associated with pregnancy-related diseases. However, the underlying regulatory mechanism of *TET3* in PE remains unclear. Here, we transfected HTR-8/

SVneo cells with siRNA targeting *TUG1* and investigated the effects of *TUG1* knockdown on the expression of *TET3* and the *DUSP* family. The results showed that downregulation of *TUG1* increased the expression of *TET3*, *DUSP2*, *DUSP4*, and *DUSP5* at both mRNA (Figure 1A) and protein (Figure 1B) levels.

We further explored the mechanisms underlying *TUG1*-mediated regulation in trophoblasts. We have previously reported that approximately 70% of *TUG1* is located in the nuclei of trophoblasts,²⁵ indicating that *TUG1* might play a key role in transcriptional regulation. Bioinformatics analysis (<http://pridb.gdcb.iastate.edu/RPISeq/references.php>) was then performed to predict potential RNA-binding proteins. As shown in Figure 1C, *TUG1* may interact with a panel of chromatin modifier *SUV39H1* (H3K9me3) in trophoblasts. To examine the potential interaction between *TUG1* and *SUV39H1*, we performed RNA immunoprecipitation (RIP) coupled with qPCR and found substantial enrichment of *SUV39H1* in HTR-8/SVneo cells (Figure 1D). Next, we constructed *TUG1*-sense/*TUG1*-antisense plasmids and performed an RNA pull-down assay. The purified ribonucleoproteins were separated using SDS-PAGE followed by silver staining (Figures 1E and 1F). Western blot analysis of affinity-purified ribonucleoproteins confirmed the interaction of *SUV39H1* with *TUG1*-sense but not with IgG (Figure 1G). Collectively, it can be concluded that *TUG1* interacts with *SUV39H1* in human trophoblasts.

As an RNA-binding protein, *SUV39H1* inactivates gene transcription by promoting histone modification, namely, H3K9me3.²⁷ We further explored the correlation between *TUG1* and *SUV39H1*. Silencing of *SUV39H1* by siRNAs significantly upregulated *TET3*, *DUSP2*, *DUSP4*, and *DUSP5* at both mRNA and protein levels (Figures 2A and 2B). Hence, we speculated that *TUG1* might repress the expression of target genes via recruitment of *SUV39H1* to the promoter region and induce H3K9me3, thereby altering the phenotype of trophoblasts in PE. Next, we performed chromatin immunoprecipitation (ChIP) coupled with qPCR. Anti-*SUV39H1* and anti-H3K9 antibodies were used to precipitate protein-DNA complexes from HTR-8/SVneo cells transfected with si*TUG1* or control siRNAs (siCon). As shown in Figure 2C, knockdown of *TUG1* suppressed the binding of *SUV39H1* to target genes and decreased the H3K9me3 level. These results reveal that *SUV39H1* can interact with the promoters of target genes, leading to H3K9 trimethylation at the promoter region.

***TET3* epigenetically regulates expression of the *DUSP* family**

TET3 is a DNA demethylase that oxidizes 5-methylcytosine to 5-hydroxymethylcytosine, which is then converted to unmethylated cytosine.^{28,29} The enzymatic activity of *TET3* is mediated by co-factors (e.g., α -ketoglutarate) generated through the tricarboxylic acid cycle and vitamin C, and by post-translational modification.³⁰ The role of *TET3* in cancer and development has been identified. Although altered *TET3* expression has been observed in preeclamptic placenta, little is known of its function in PE.³¹

As a DNA-binding protein, *TET3* activates gene transcription by promoting DNA demethylation.²⁹ We first investigated whether aberrant

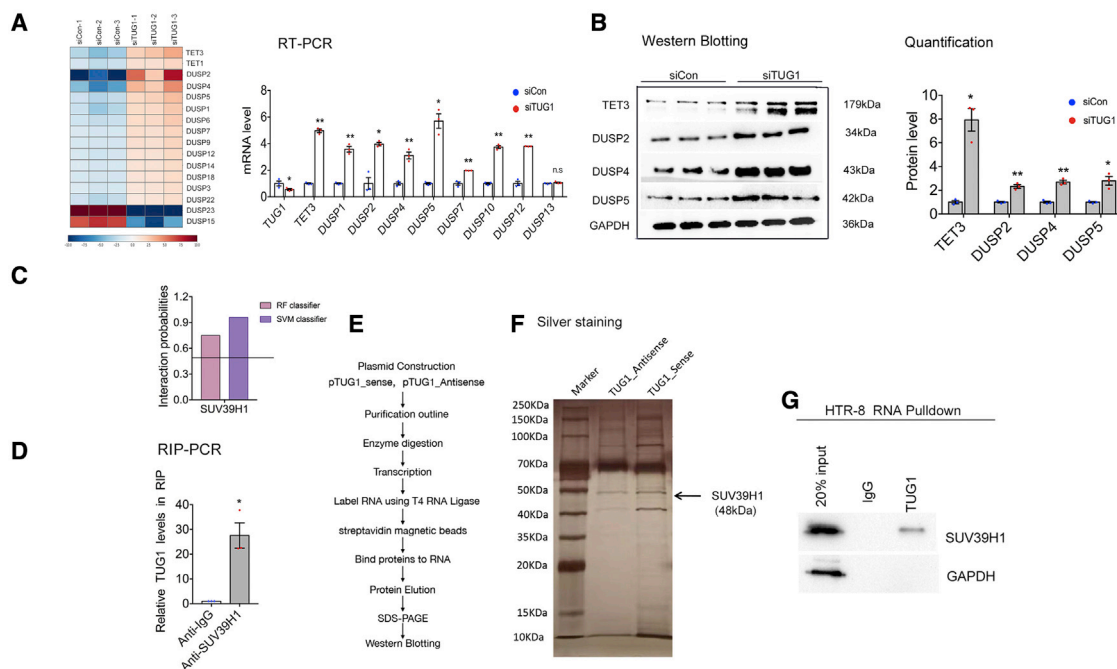


Figure 1. TUG1 inhibits the expression of TET3 and the DUSP family

(A) Mean-centered, hierarchical clustering of transcripts altered in siCon-treated cells and siRNA-TUG1-treated trophoblasts (left panel). HTR-8/SVneo trophoblasts were transfected with siCon or siTUG1. Quantitative real-time PCR was used to measure the mRNA expression of genes at 48 h post-transfection (right panel). (B) Protein expression was detected using western blot at 48 h after transfection. (C) Bioinformatics analysis predicted the interaction possibility of TUG1. A probability of >0.5 was considered positive. The RPISeq prediction was based on support vector machine or random forest. (D) RIP assay was performed, followed by quantitative real-time PCR analysis of co-precipitated RNA. (E) Schematic outline of the purification of TUG1-associated ribonucleoproteins and protein identification. (F) Silver staining gel with a protein molecular weight marker (in kilodaltons) labeled on the left. Black arrows indicate the protein bands of SUV39H1. (G) *In vitro*-transcribed pull-down assay revealed that TUG1 recruited SUV39H1 protein in HTR-8/SVneo cells, but not GAPDH (negative control). All experiments were repeated at least three times.

expression of TET3 would affect the expression of the DUSP family. Intriguingly, TET3 knockdown markedly decreased the cellular expression of DUSP2, DUSP4, and DUSP5 (Figures 3A and 3B). Next, we examined whether TET3 knockdown altered promoter methylation in the DUSP2, DUSP4, and DUSP5 genes. The genome-wide single-nucleotide resolution of DNA methylation (GEO: GSE117190)³² in human uterine cells with TET3 deficiency showed increased methylation of the DUSP2, DUSP4, and DUSP5 promoters (Data S6).

To determine whether TET3 knockdown in HTR-8/SVneo cells would increase methylation of the DUSP2, DUSP4, and DUSP5 promoters, we performed targeted bisulfite sequencing on the basis of the next-generation sequencing platform to validate the methylation status. As shown in Figures 3C–3K, the methylation level of the CpGs in the DUSP2, DUSP4, and DUSP5 promoters was significantly increased. Pyrosequencing was used to detect promoter demethylation of these genes (Data S5). In addition, the placental tissues of healthy pregnant women and PE patients were collected, and targeted bisulfite sequencing was performed to characterize the methylation status of the CpG sites in the DUSP2, DUSP4, and DUSP5 promoters. As shown in Figures 3L–3N, the methylation level of DUSP2 and DUSP4 promoters in pre-eclamptic placenta was significantly increased compared with controls. These data suggest that TET3 positively regulates the expression of

DUSP2, DUSP4, and DUSP5 in EVT, likely in part by increasing demethylation at specific CpG sites in the promoter regions of these genes.

Hypoxia-induced miR-218 acts as a FOXP1 sponge and inhibits its expression

Insufficient uteroplacental oxygenation is implicated in the molecular events that lead to the development of PE.^{7,33} Fang et al.³⁴ found that hypoxia increased the expression of miRNA-218 by promoting its binding to transcription factor HIF-1 α , resulting in the inhibition of trophoblast proliferation and invasion. Here, we investigated whether hypoxia regulated the expression of miR-218. The exposure of HTR-8/SVneo cells to 0.5% O₂ for 24 h significantly increased the mRNA expression of HIF-1 α and miR-218 (Figure 4A). Then, ChIP was performed to determine whether hypoxia regulated miR-218 expression by promoting the binding of HIF-1 α to the promoter of miR-218. As shown in Figures 4B and 4C, transcription factor HIF-1 α bound to the promoter region of miR-218 to stimulate its expression.

Bioinformatics analysis (<http://bibiserv.techfak.uni-bielefeld.de/rnahybrid/>) predicted three binding sites of miR-218 in the 3' UTR of FOXP1 (Figure 4D). The binding between miR-218 and FOXP1 might lead to FOXP1 mRNA degradation and/or translational repression. To

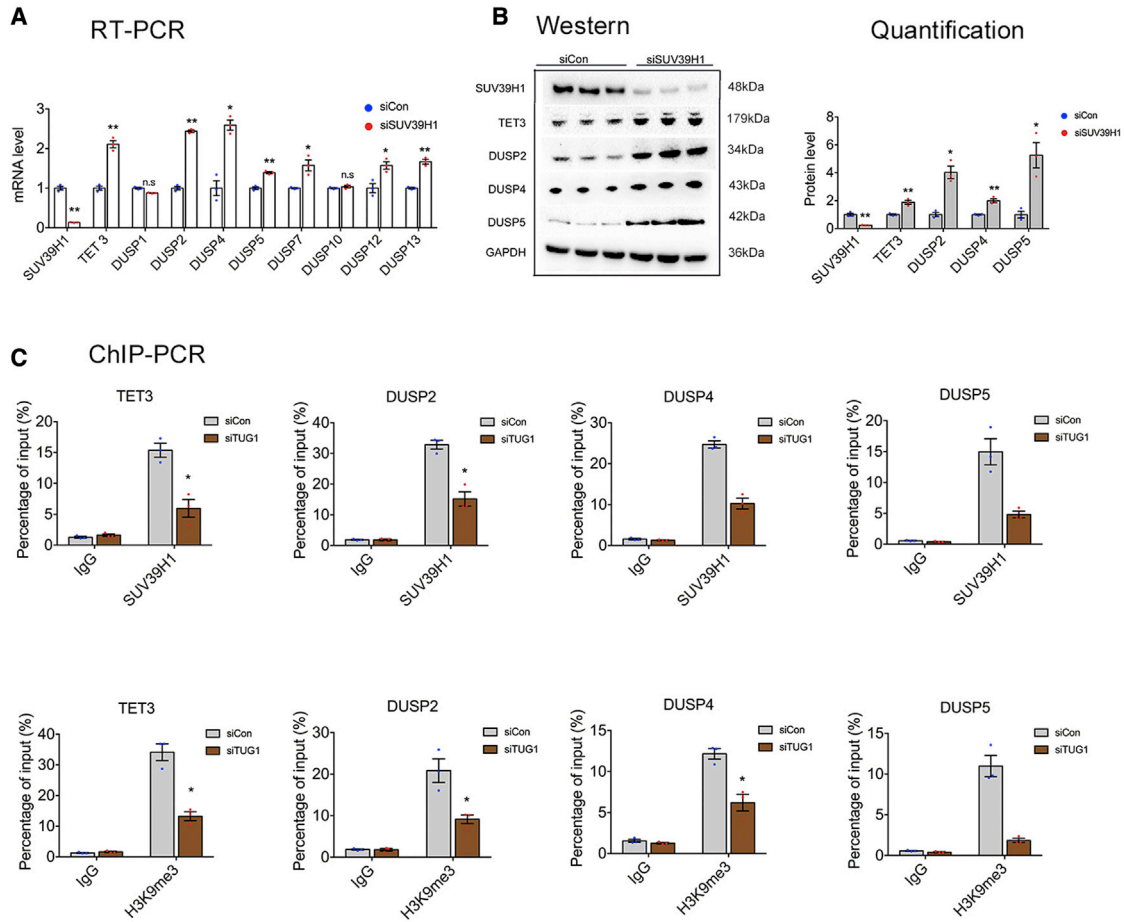


Figure 2. TUG1 epigenetically regulates TET3 and the DUSP family by recruiting SUV39H1

(A and B) HTR-8/SVneo trophoblasts were transfected with siCon or siSUV39H1 for 48 h (n = 3). The silencing of SUV39H1 promoted the expression of downstream genes at both mRNA (A) and protein (B) levels. (C) HTR-8/SVneo cells were transfected with siTUG1 or siCon. ChIP coupled with qPCR was performed at 48 h after transfection. The mean relative enrichment of SUV39H1 over input after normalization against IgG (negative control) is shown (n = 3). ChIP coupled with qPCR showed that SUV39H1 and H3K9me3 were enriched in the promoter regions of *TET3*, *DUSP2*, *DUSP4*, and *DUSP5*, and the enrichment was decreased after silencing of *TUG1*. Error bars indicate mean \pm SEM. *p < 0.05 and **p < 0.01.

validate this concept, we cultured HTR-8/SVneo cells under 0.5% O₂ for 24 h. The mRNA expression of FOXP1 was significantly decreased compared with controls (Figure 4F). Then, 293 and HTR-8/SVneo cells were co-transfected with the 3' UTR of FOXP1 (or the mutant 3' UTR of FOXP1) and miR-218. The relative luciferase activity of the reporters containing the 3' UTR of FOXP1 was significantly reduced in the groups transfected with miR-218 (Figure 4E). In contrast, the luciferase activity of the reporters containing mutant 3' UTR of FOXP1 had no effect on cells transfected with miR-218 (Figure 4E). After 24 h exposure to 0.5% O₂, the mRNA expression of FOXP1 and *TUG1* in HTR-8/SVneo cells was significantly decreased, while that of *TET3*, *DUSP2*, *DUSP4*, and *DUSP5* was increased (Figure 4F). The above data imply that miR-218 binds to the 3' UTR of FOXP1 and inhibits its expression.

The effects of miR-218 knockdown by inhibitors on the expression of FOXP1, *TUG1*, *TET3*, and the *DUSP* family in HTR-8/SVneo cells

were explored. Downregulation of miR-218 increased the expression of FOXP1 and *TUG1* and decreased expression of *TET3*, *DUSP2*, *DUSP4*, and *DUSP5* at both mRNA (Figure 5A) and protein (Figures 5B and 5C) levels, while overexpression of miR-218 by miR-218 mimics significantly upregulated FOXP1 and *TUG1* and downregulated *TET3*, *DUSP2*, *DUSP4*, and *DUSP5* at both mRNA and protein levels (Figures 5E–5G). These findings suggest that miR-218 negatively regulates the expression of FOXP1 and downregulates *TUG1*, *TET3*, *DUSP2*, *DUSP4*, and *DUSP5* in HTR-8/SVneo cells.

Subsequently, a rescue experiment was performed to determine whether the regulation was mediated by miR-218. As expected, the transfection of cells overexpressing miR-218 with pFOXP1 increased the expression of FOXP1 (Figures 5G and 5H). However, knockdown of FOXP1 in cells transfected with miR-218 inhibitors eliminated the effects of miR-218 deficiency on the upregulation of FOXP1 (Figures

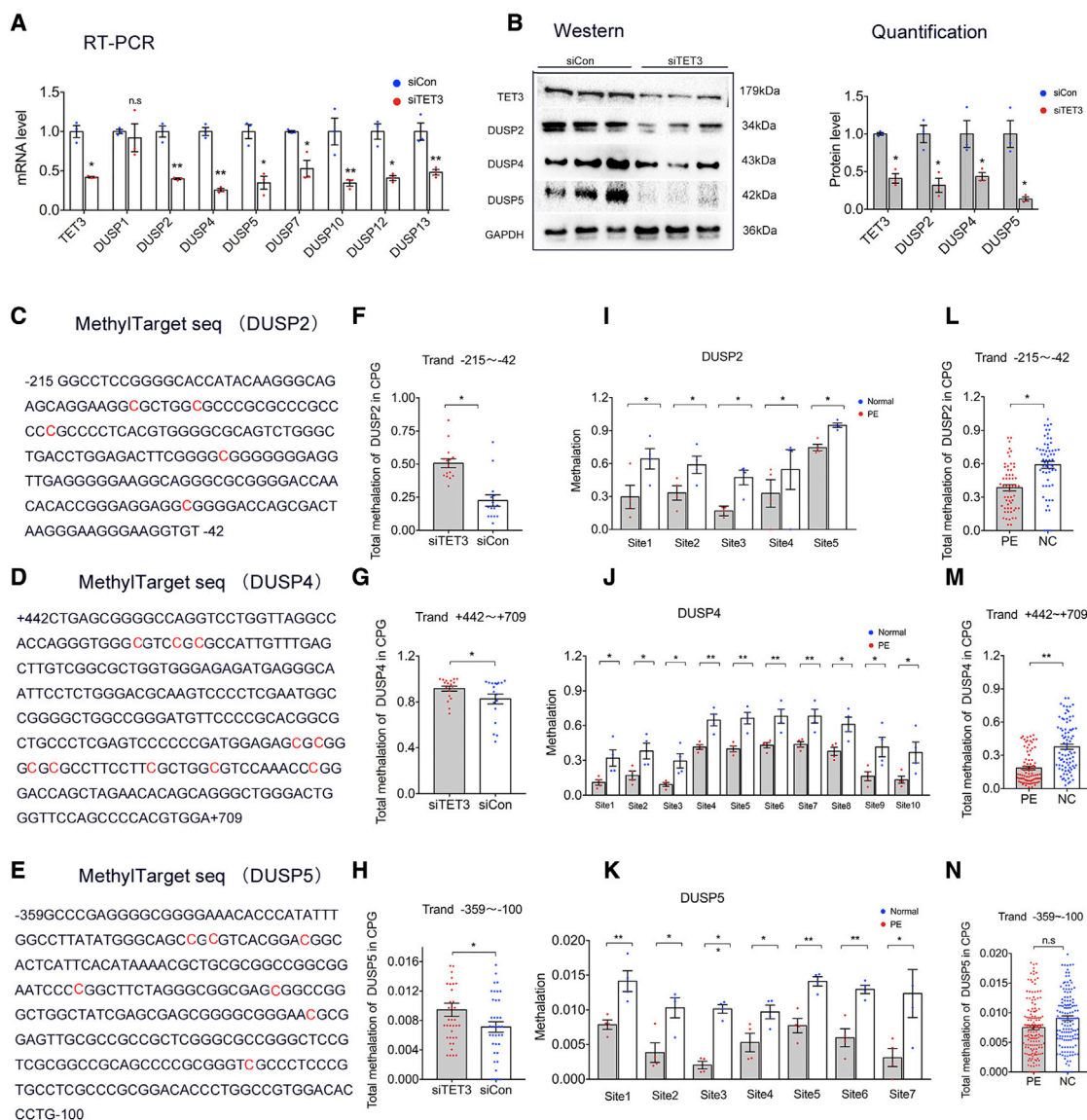


Figure 3. TET3-dependent epigenetic regulation of the DUSP family

(A and B) mRNA and protein expression of genes of interest in HTR-8/SVneo cells transfected siTET3 or siCon was measured using quantitative real-time PCR and western blot, respectively. Total RNA and protein were isolated at 48 h after transfection ($n = 3$). (C–E) Sequences of critical transcription regulatory regions of DUSP2, DUSP4, and DUSP5. The number indicates the position of the nucleotide relative to the transcription initiation site. Differentially methylated cytosine residues are highlighted in red. HTR-8/SVneo cells were transfected with siTET3 or siCon. MethyTarget sequencing analysis was performed at 48 h post-transfection. The methylation levels of the CpG sites in the DUSP2, DUSP4, and DUSP5 genes are shown (F–H) ($n = 3$). Genomic DNA was extracted from human placental tissues ($n = 4$ per group) and analyzed using MethyTarget sequencing. The promoter methylation levels of the CpG sites in the DUSP2, DUSP4, and DUSP5 genes are shown (I–K). The total promoter methylation levels of the CpG sites in the DUSP2, DUSP4, and DUSP5 genes are presented (L–N). Error bars indicate mean \pm SEM. * $p < 0.05$ and ** $p < 0.01$.

5K–5N). These findings indicate that miR-218 regulates the expression of FOXP1 *in vitro* at the post-transcriptional level.

Transcription factor FOXP1 activates TUG1 and inhibits the expression of TET3 and the DUSP family

The expression of most human lncRNAs is mediated by various transcription factors. The JASPAR database (<http://jaspar2014.genereg.net>)

was used to identify potential factors that may activate or inactivate the transcription of TUG1. As shown in Figure 6E, there were several FOXP1-binding sites in the promoter region of TUG1, implying that TUG1 might be regulated by FOXP1 in trophoblasts. Then, we transfected HTR-8/SVneo cells with designated plasmids and siRNAs to either upregulate or downregulate FOXP1. The level of TUG1 was significantly increased in cells overexpressing FOXP1,

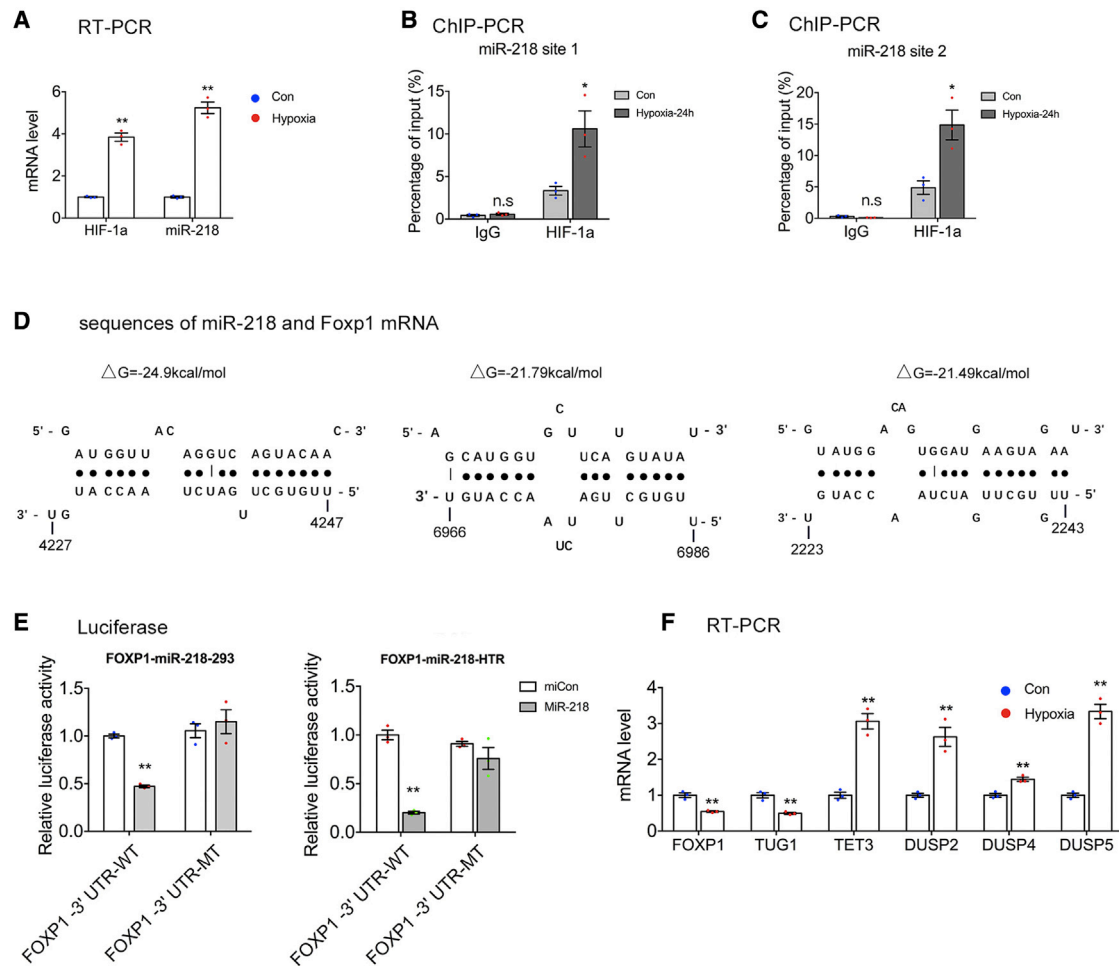


Figure 4. Hypoxia-induced miR-218 inhibits the expression of FOXP1

(A) HTR-8/SVneo cells were cultured under hypoxic conditions (0.5% oxygen) for 24 h. Quantitative real-time PCR was used to detect the mRNA expressions of HIF-1 α and miR-218. (B and C) ChIP assay showed that HIF-1 α was enriched at two sites of the promoter region of miR-218, and the enrichment was increased in HTR-8/SVneo cells exposed to 0.5% oxygen for 24 h. (D) Predicted base-pairing interaction between FOXP1 mRNA and miR-218. (E) Luciferase reporter assay was used to detect the interaction between miR-218 and FOXP1 in 293 and HTR-8/SVneo cells. Relative luciferase activity was normalized to Renilla luciferase activity. (F) Quantitative real-time PCR of genes of interest in HTR-8/SVneo cells exposed to 0.5% oxygen for 24 h (n = 3). Error bars indicate mean \pm SEM. *p < 0.05 and **p < 0.01.

and the expression of *TET3*, *DUSP2*, *DUSP4*, and *DUSP5* was also greatly increased (Figures 6A and 6B). An opposite trend was observed in cells with insufficient FOXP1 expression (Figures 6C and 6D).

Next, we performed luciferase reporter assay (Figure 6F) and ChIP assay (Figure 6G) to examine whether *TUG1* regulation was mediated by FOXP1. As expected, FOXP1 knockdown significantly reduced the binding of FOXP1 to the *TUG1* promoter, which was consistent with the aforementioned data showing the physical interaction between FOXP1 and the *TUG1* promoter. These findings indicated that FOXP1 bound to the promoter region of the *TUG1* gene to stimulate its expression. Taken together, these results support the statement that the hypoxia-miR-218/FOXP1/*TUG1* axis regulates the function of trophoblasts in a cell-autonomous manner (Figure 6H).

Expression of *TUG1*, *TET3*, and the *DUSP* family was significantly changed in rats with L-NAME-induced PE and human preeclamptic placenta

We further measured the expression of *TUG1*, *TET3*, and the *DUSP* family in rats with L-NAME-induced PE (Figure 7A). The mean systolic blood pressure (SBP) of the control group on gestational day (GD) 8 was 110.77 ± 4.12 mm Hg, and that of pregnant rats awaiting L-NAME treatment was 146.67 ± 6.94 mm Hg (p < 0.05). After L-NAME treatment, the mean SBP of rats with L-NAME-induced PE was increased on GD 8 and maintained until GD 18.5. The mean SBP of the PE group was significantly increased compared with the controls (Figure 7B). The average weights of the fetuses and placental tissues of the PE group were also significantly lower than those of healthy controls (Figure 7C). Immunohistochemistry analysis showed that the protein

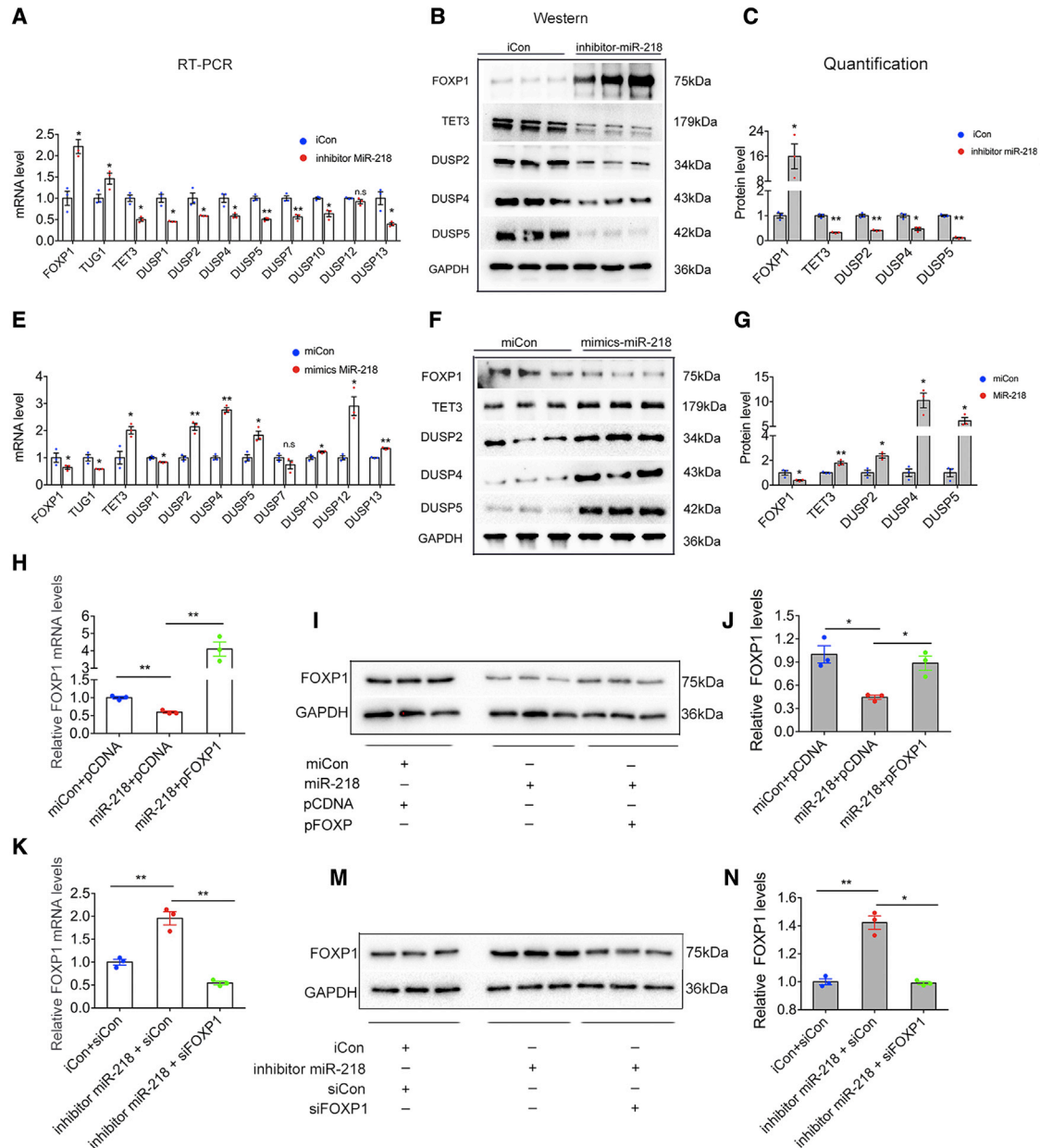


Figure 5. MiR-218 regulates the expression of FOXP1 at the post-transcriptional level

(A–C) Quantitative real-time PCR and western blot analysis of genes of interest in HTR-8/SVneo cells transfected with iCon or miR-218 inhibitor for 48 h ($n = 3$). (E–G) Quantitative real-time PCR and western blot analysis of genes of interest in HTR-8/SVneo cells transfected with miCon or mimics miR-218 for 48 h ($n = 3$). (H–J) HTR-8/SVneo cells were transfected with miCon + pCDNA, miR-218 + pCDNA, or miR-218 + pFOXP1 for 48 h. Total RNA and protein were extracted and analyzed using quantitative real-time PCR (left panel) and western blot (right panels), respectively ($n = 3$). (K–N) HTR-8/SVneo cells were transfected with iCon + siCon, inhibitor miR-218 + siCon, or inhibitor miR-218 + siFOXP1 for 48 h. Total RNA and protein were isolated and analyzed using quantitative real-time PCR (left panel) and western blot (right panels), respectively ($n = 3$). Data are from three independent experiments. Error bars indicate mean \pm SEM. * $p < 0.05$ and ** $p < 0.01$.

expression of TET3, DUSP2, and DUSP5 in the placental tissues of PE rats was increased, while FOXP1 was downregulated (Figure 7D; Data S7). The results of the animal study were in line with those observed in HTR-8/SVneo cells.

In addition, we examined the correlations of the mRNA levels of these genes in human preclampsic placenta. The mRNA levels of *TUG1* and TET3, *TUG1* and DUSP2, *TUG1* and DUSP4, and *TUG1* and DUSP5 were significantly and negatively correlated (Figure 7E). A

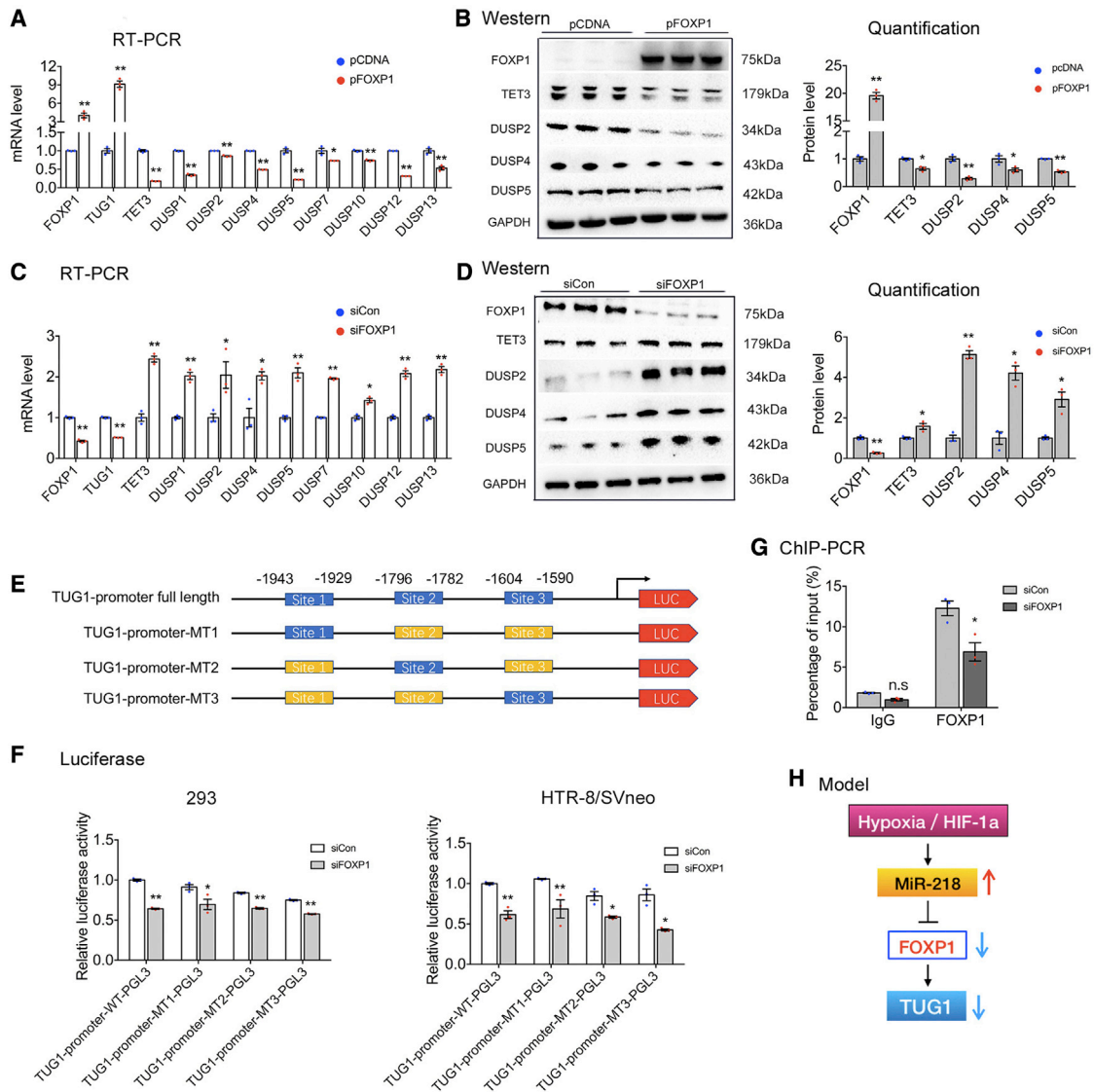


Figure 6. Transcription factor FOXP1 activates the transcription of TUG1 and inhibits the expression of TET3 and the DUSP family. (A and B) Quantitative real-time PCR and western blot were performed to assess the expression of target genes in HTR-8/SVneo cells transfected FOXP1 plasmid (pFOXP1) or empty vector (pCDNA) for 48 h (n = 3). (C and D) Quantitative real-time PCR and western blot analysis of target genes in HTR-8/SVneo cells transfected with siCon or siTET3 for 48 h (n = 3). The putative binding sites of FOXP1 in the TUG1 promoter were predicted by JASPAR. The potential binding sites were highlighted in blue (E). Luciferase reporter assay (F) was used to determine the interaction between FOXP1 and TUG1. The luciferase activity was normalized to Renilla luciferase activity. (G) HTR-8/SVneo cells were transfected with siFOXP1 or siCon for 48 h. ChIP coupled with qPCR was then performed. The mean relative enrichment of FOXP1 over input after normalization against IgG (negative control) is shown (n = 3). (H) Upstream regulation of TUG1. Error bars indicate mean ± SEM. *p < 0.05 and **p < 0.01.

significant positive correlation between the levels of FOXP1 and TUG1 was also observed (Figure 7E). We further analyzed the mRNA expression of TET3 and its target genes, DUSP2, DUSP4, and DUSP5, in preeclamptic placenta and matched normal placental tissues. As shown in Figure 7E, the expression of TET3 was positively correlated with the levels of all target genes, confirming the *in vitro* results that TUG1 knockdown in trophoblasts increased the expression of TET3, DUSP2, DUSP4, and DUSP5, and regulation by TUG1 was at the epigenetic level. Collectively, these data implicate

FOXP1-mediated regulation of TUG1 in the pathogenesis of PE. The potential regulatory pathway is shown in Figure 8. Whether TUG1 would regulate other genes or pathways in placental trophoblasts warrants further investigation.

DISCUSSION

PE is a common obstetric complication among pregnant women that may lead to maternal and fetal morbidity and mortality.³⁵ Current treatments for PE are not satisfactory and the only way to prevent

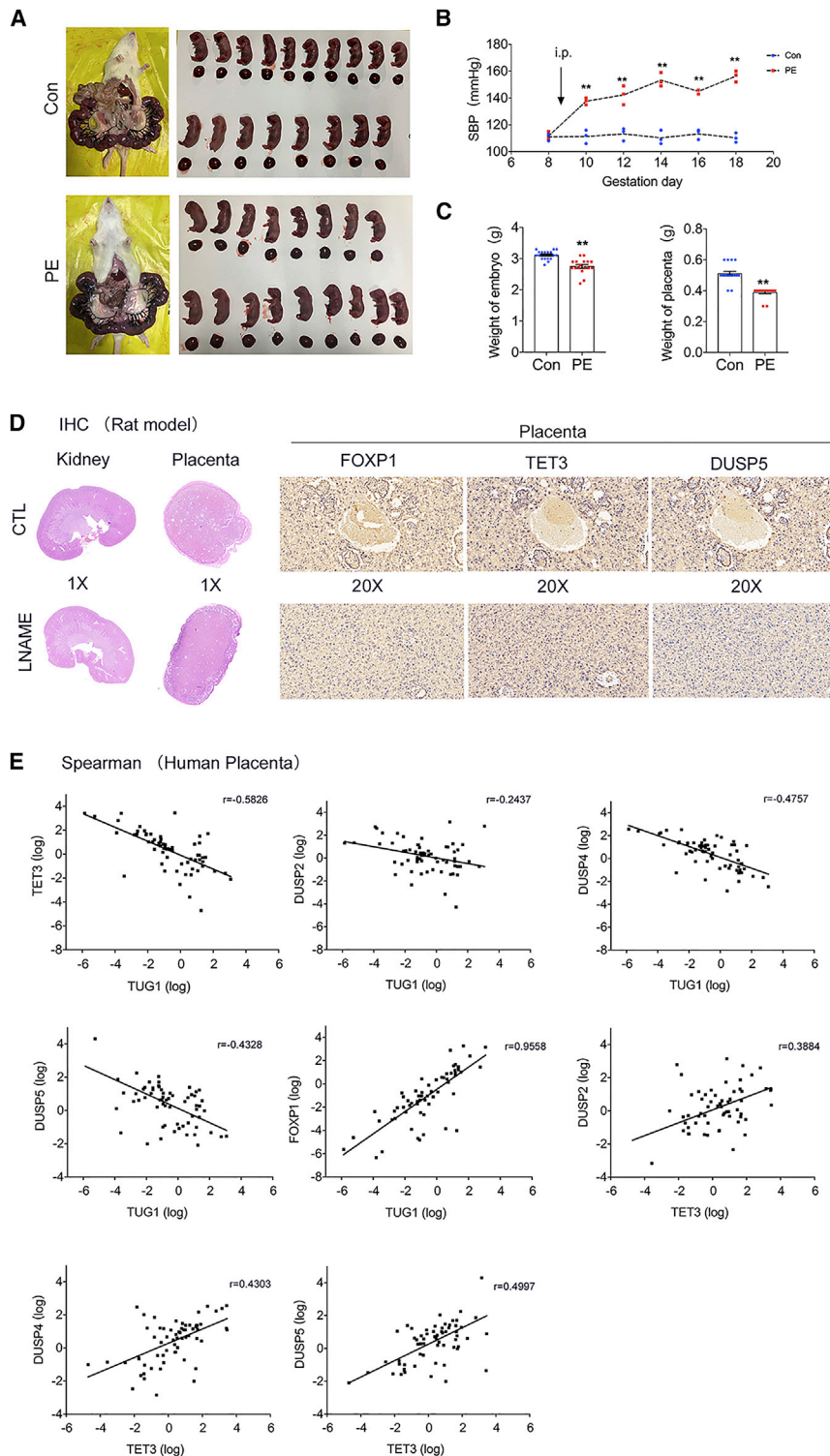


Figure 7. Altered expression of *TUG1*, *TET3*, and the *DUSP* family in rats with L-NAME-induced PE and human preeclamptic placenta

(A) L-NAME or normal saline was intraperitoneally injected into pregnant rats. The embryos and placental tissues were collected, counted, and weighed. (B) Changes in SBP in the two groups. ** $p < 0.001$ compared with SBP on GD 8 before intraperitoneal injection of L-NAME or normal saline. (C) The average weights of the embryos and placental tissues of the control and L-NAME groups were measured. (D) Four images on the left show representative photomicrographs of hematoxylin-eosin-stained kidney and placenta sections of saline- or L-NAME-treated rats on GD 18.5. Six images on the right show immunohistochemistry staining of placental tissues using antibodies against FOXP1, TET3, and DUSP5. Magnification, 20 \times ; scale bar, 100 μ m. (E) Spearman's correlation analysis revealed negative correlations between the expression of TUG1 and TET3 and between TUG1 and its target genes (DUSP2, DUSP4, and DUSP5). Positive correlations between mRNA expression of TUG1 and FOXP1 and between TET3 and DUSP2, DUSP4, and DUSP5 were found in 64 paired preeclamptic and control placental tissues. Error bars indicate mean \pm SEM. * $p < 0.05$ and ** $p < 0.01$.

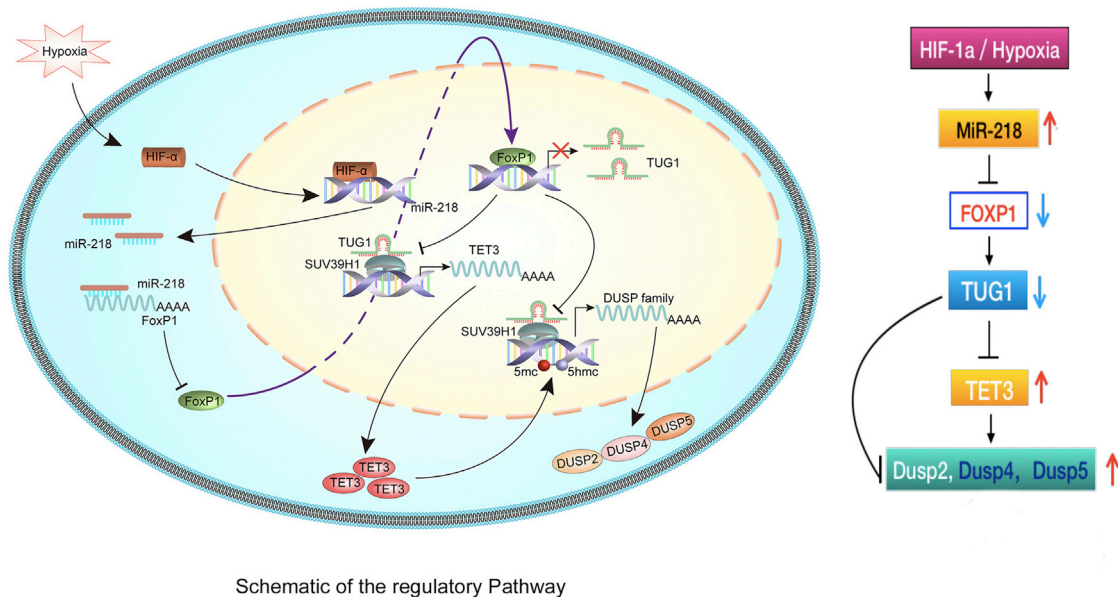


Figure 8. Schematic of the regulatory pathway

the progression of PE is to induce delivery.³⁶ Hence, it is of significant importance to comprehensively understand the pathogenic mechanisms of PE and to identify new prognostic factors. Increasing evidence has shown the involvement of lncRNAs in cell development and human diseases.^{37,38} lncRNAs are also involved in human normal development, cell differentiation, RNA decay, genomic imprinting, chromatin modification, and regulation of sponge-like miRNAs.^{39,40} Our previous study demonstrated that *TUG1* was markedly downregulated in the placental tissues of PE patients.²⁵ Moreover, *TUG1* might result in SAR impairment in PE. Thus, we proposed that *TUG1* might play an essential role in the progression of PE. Here, we investigated the regulatory mechanisms of *TUG1* in the development of PE.

The TET proteins are a group of DNA demethylases that oxidize 5-methylcytosine to 5-hydroxymethylcytosine.⁴¹ The DUSP family is characterized by highly conserved amino acid sequences, while different DUSP members may have different functions.⁴² The DUSP family is implicated in a variety of biological processes. DUSP9 maintains the stem cell-like characteristics of cancer cells and is related to the development of breast cancer.⁴³ Importantly, the biological functions of lncRNAs depend largely on their subcellular localization.⁴⁴ We have shown that most *TUG1* is located in the nuclei of trophoblasts, indicating its potential function. In this study, RNA sequencing analysis, gene expression profiles, and *in vitro* cell function experiments showed that TET3 and the DUSP family were negatively regulated by *TUG1*. Moreover, the expression of TET3 and the DUSP genes were significantly correlated in PE. One of the pathogenesis of preeclampsia has been confirmed to be related to abnormal changes in methylation.^{45,46} Thus, we suspect that the occurrence of preeclampsia may be

related to TET3-DUSPs in some way. The genome-wide single-nucleotide resolution of DNA methylation, pyrosequencing analysis, and bisulfite sequencing indicated that TET3 regulated the expression of the DUSP genes partially by increasing demethylation at specific CpGs in their promoter regions. These results were confirmed in the rat model of L-NAME-induced PE. Our resulting data demonstrated that TET3 positively regulates the expression of DUSP2, DUSP4, and DUSP5 in EVT, likely in part by increasing demethylation at specific CpG sites in the promoter regions of these genes. We believe that the molecular and functional interaction between TET3 and the DUSPs characterized in this report represents a critical mechanism in the impairment of spiral artery remodeling in PE.

Epigenetic regulation plays a crucial role in various diseases, including PE.⁴⁷ Approximately 70% of *TUG1* is located in the nuclei of trophoblasts, suggesting that *TUG1* may play an essential role in epigenetic regulation. To further investigate how *TUG1* regulated TET3 and the DUSP family, bioinformatics analysis and RIP coupled with qPCR were performed. Our results showed a binding preference of *TUG1* to SUV39H1 in human trophoblasts. As previously reported, genes recruit the H3K9MTases SUV39H1 to the genome, resulting in the enrichment of H3K9me2/me3 and therefore promoting the development of many cancers.⁴⁸ However, little is known about the roles of SUV39H1 and SUV39H1-associated H3K9me3 modification in PE. In the present study, silencing of SUV39H1 upregulated both TET3 and the DUSP family. In addition, *TUG1* knockdown suppressed the binding of SUV39H1 and decreased the H3K9me3 level. The above findings indicate that *TUG1* might regulate the progression of PE via mediating the expression of TET3 and the DUSP family by recruiting SUV39H1.

The expression of human lncRNAs is mediated by various transcription factors. FOXP1 is an evolutionally conserved transcription factor that binds to highly conserved regions of the DNA and is required for the proper development of pulmonary, neural, intestinal, cardiovascular, and lymphoid tissues.⁴⁹ Here, the JASPAR database was used to identify the potential upstream targets of *TUG1* in PE. The results showed that there were several binding sites of FOXP1 in the promoter region of *TUG1*. Also, FOXP1 knockdown significantly decreased the expression of *TUG1* but increased the expression of TET3 and the DUSP family. Furthermore, luciferase reporter assay and ChIP assay indicated that FOXP1 bound to the promoter region of *TUG1* to stimulate its expression.

The upregulation of hypoxia-inducible transcription factors and hypoxia-related genes in the placenta suggests that hypoxia is essential for the pathogenesis of PE.³³ HIF-1 α , a marker of cellular oxygen deprivation, is highly expressed in proliferative trophoblasts and in the placenta of PE patients.⁵⁰ A previous study reported that miR-218 promoted trophoblast invasion, induced EVT-to-eEVT differentiation, and accelerated SAR.⁵¹ In this study, we identified HIF-1 α as an interactor of miR-218. The binding preference of these hypoxia-inducible factors under hypoxic conditions was confirmed by ChIP assay.

Recently, considerable attention has been focused on the sponge effect of miRNA.⁵² miRNAs regulate gene expression by directly binding mRNAs and subsequently suppressing mRNA translation or inducing mRNA degradation.⁵³ Here, we predicted the binding sites of miR-218 in the 3' UTR of the FOXP1 mRNA, indicating that miR-218 might repress the translation of FOXP1 mRNA and/or induce the degradation of FOXP1 mRNA. Moreover, the expression of FOXP1 was significantly decreased under hypoxic conditions. Further RT-PCR and luciferase reporter assay confirmed the binding of miR-218 to FOXP1. Our data implied that miR-218 negatively regulated the expression of FOXP1 and decreased the levels of *TUG1*, TET3, DUSP2, DUSP4, and DUSP5 in trophoblasts, indicating that hypoxia-induced HIF-1 α mediated the expression of FOXP1 and its downstream genes through a miR-218-dependent mechanism.

Finally, we investigated the correlations of the expression of these genes in human placenta. The level of *TUG1* was significantly and negatively correlated with the expression of TET3, DUSP2, DUSP4, and DUSP5. A significant positive correlation between the expression of *TUG1* and FOXP1 was also observed. Furthermore, the TET3 expression was positively correlated with the levels of DUSP2, DUSP4, and DUSP5.

In conclusion, this study provides novel evidence supporting lncRNA *TUG1* as a link between hypoxia and the development of PE. Our results suggest that hypoxia-induced-HIF-1 α regulated miR-218, which then inhibited the expression of the transcription factor FOXP1. Moreover, FOXP1 activated *TUG1*, which epigenetically inhibited the expression of TET3 and the DUSP family via recruitment of SUV39H1. These findings highlight the importance of *TUG1*-medi-

ated regulatory network in PE and provide new insights into the potential therapeutic targets for PE.

MATERIALS AND METHODS

Establishment of animal model with L-NAME

Pregnant Sprague-Dawley (SD) rats (8 weeks old) were obtained from the Experimental Animal Research Institute of Nanjing Medical University and housed in a controlled environment (temperature 21 \pm 3°C, 12 h/12 h light/dark cycle). All rats had free access to water and standard food before experiments. This study approved by the Animal Care and Use Committee of Nanjing Medical University in accordance with the National Institutes of Health Guidelines for Use and Care of Animals.

Pregnant SD rats were randomly separated into two groups, an L-NAME group and a control group. Rats in the L-NAME group received intraperitoneal injections of L-NAME (125 mg/kg body weight) on gestational days 9.5, 10.5, 11.5, 12.5, 13.5, 14.5, and 15.5. Rats in the control group were administered phosphate-buffered saline (1 mL/kg body weight) following the same procedure.

Blood pressure (BP) was measured on GDs 8.5, 10.5, 12.5, 14.5, and 16.5 using a programmed electro-sphygmomanometer (BP-98A; Softron, Tokyo, Japan) according to the tail-cuff method. Blood was obtained from the orbital sinus of each rat. The urine samples were also collected. On GD 16.5, rats were euthanized. Placentas and fetuses were dried and weighed.

Cell culture and transfections of cell lines

We selected cell lines that were related to pregnancy. HTR-8/SVneo cells were generously furnished by Prof. Charles Graham (Queen's University, Kingston, ON, Canada). The 293T cell lines were purchased from the Institute of the Chinese Academy of Sciences (Shanghai, China). HTR-8 and 293T cells were maintained in RPMI 1640 medium (Gibco, Nanjing, China) supplemented with 10% fetal bovine serum (FBS) (Gibco, BRL, Invitrogen, Carlsbad, CA) and antibiotics (100 μ g/mL streptomycin and 100 U/mL penicillin G). All cell lines were cultured in humidified air at 37°C and 5% CO₂. For hypoxia treatment, cells were exposed to 0.5% O₂ in a hypoxic incubator (BioSpherix, Redfield, NY) for the indicated time.

For transfection of suspended HTR-8/SVneo cells, a volume of 1–2 μ L Lipofectamine 3000 transfection reagent was mixed with 25 μ L OPTI-MEM. Meanwhile, 20 pmol siRNAs were mixed with 25 μ L OPTI-MEM. After 5 min, the mixture containing siRNAs and Lipofectamine 3000 reagent was mixed and placed at room temperature for 5–10 min. Then, 50 μ L transfection solution was added to re-suspend cells (6 \times 10⁴ cells per well in 24-well plates). After 10 min incubation at room temperature, 450 μ L fresh culture medium was added to suspended cells, which were then transferred to the culture plate.

For on-plate transfection of primary trophoblasts, cells were seeded in six-well plates (6 \times 10⁴ per well). After 6 h, on-plated transfection was

performed. A volume of 240 μL OPTI-MEM was incubated with 10 μL siRNAs (100 pmol) for 5 min. Meanwhile, 240 μL OPTI-MEM was mixed with 10 μL Lipofectamine 3000 reagent and placed at room temperature for 5 min. Then, the mixture containing siRNAs and Lipofectamine 3000 reagent was mixed and placed at room temperature for 20 min. Subsequently, 500 μL total solution was added to each well of the six-well plate. After 6 h of transfection, transfected solution was replaced by fresh culture medium. HTR-8/SVneo and 293 cells were seeded in six-well plates and transfected with 40 nM miR-218 inhibitor, miR-218 mimic, or corresponding controls (RiboBio, Guangzhou, China) for 48 h. Cells were also plated in six-well plates and transfected with 3 μg plasmid (vector, pcDNA3.1 + FOXP1, and pcDNA3.1 + TET3).

Placenta samples collection

Placental tissue samples were obtained from 64 PE patients and 64 paired healthy controls who underwent cesarean section at the First Affiliated Hospital of Nanjing Medical University from 2017 to 2019. All placental tissues were washed with sterile saline and stored in liquid nitrogen. The clinicopathological characteristics of healthy pregnant women and PE patients are summarized in [Table S1](#) (published by Zhang et al.⁵⁴). The study protocol was approved by the ethics committee of the First Affiliated Hospital of Nanjing Medical University. All subjects provided written informed consent.

Quantitative real-time PCR

This experiment was performed as described by Geng et al.⁵⁵ with minor modifications. Briefly, total RNA was extracted from placental tissues or cultured cells using PureLink RNA Mini Kit (catalog no. 12183018A; Ambion). Total RNA (0.8 μg) was reverse-transcribed to cDNA in a reaction volume of 10 μL using PrimeScript RT Reagent Kit (catalog no. RR037A; Takara, Tokyo, Japan). Quantitative real-time PCR was performed using SYBR Premix Ex Taq (Takara, Dalian, China) and the ABI 7500 system. The expressions of target genes was normalized to those of housekeeping genes ACTB and GAPDH. The sequences of PCR primers for rat and human tissues were summarized in [Data S1](#).

Transcriptome sequencing analysis

Transcriptome sequencing analysis was performed as described in our previous study.²⁵

RNA immunoprecipitation assay (RIP)

RIP was performed as previously described.²⁵

Chromatin immunoprecipitation assay (ChIP)

ChIP was performed as previously described by Xu et al.⁵⁶

Western blotting

Protein expression was measured using western blot as previously described.⁵⁶ Protein samples (5–10 μL) were loaded onto a 10% SDS gel and analyzed using western blot. GAPDH was used as an internal control. The antibodies used in this experiment and the conditions of western blot are shown in [Table S2](#). The intensity of protein

bands was quantified using Quantity One software (Bio-Rad, Hercules, CA). The uncropped western blot images are shown in [Data S2](#).

Luciferase reporter assay

As previously described by Zhang et al.,⁵⁷ the amplified cDNA fragments of the *TUG1* and *FOXP1* promoters were subcloned into the downstream of the luciferase gene in the pGL3 plasmid. The mutant plasmids (i.e., pGL3-*FOXP1*-3'-UTR-MUT and pGL3-*TUG1*-MUT) were obtained using Platinum Pfx DNA Polymerase. The luciferase activity was determined using the Dual-Luciferase Reporter Assay System (Promega, Madison, WI). In brief, HTR-8/SVneo cells (1×10^5 per well) were plated in 24-well plates for 36 h. At 48 h post-transfection, cells were lysed and collected. The relative luciferase activity was normalized to Renilla luciferase activity. The binding sites of miR-218 in the 3'-UTR of *FOXP1* are shown in [Table S3](#) and [Data S3](#).

Targeted bisulfite sequencing

MethylTarget sequencing analysis was performed by Shanghai Gene-sky Biotechnology Company (Shanghai, China). Primers were designed and validated using Methylation Primer software using bisulfite-converted DNA. The primer sets were designed to flank each targeted CpG site in 200 nt regions ([Table S4](#)). After PCR amplification using HotStarTaq Polymerase Kit (Takara) and library construction, samples were sequenced using the MiSeq Benchtop Sequencer (Illumina) following the paired-end sequencing protocol. Detailed experimental procedures are shown in [Data S4](#).

RNA pull-down assay

Briefly, RNA transcription *in vitro* was performed using mMES-SAGE mMACHINE T7 Transcription Kit according to the manufacturer's instructions (catalog no. AM1344; Invitrogen). Then, *TUG1* RNAs were labeled with desthiobiotinylation using the Pierce RNA 3' End Desthiobiotinylation Kit (catalog no. 20164, Magnetic RNA-Protein Pull-Down Kit, Components; Thermo Fisher Scientific). RNA pull-down assays were conducted using the Pierce Magnetic RNA-Protein Pull-Down Kit according to the manufacturer's instructions (catalog no. 20164, Magnetic RNA-Protein Pull-Down Kit). After elution of lncRNA-interacting proteins, they were subjected to western blotting analysis. Detailed process of RNA pull-down assay are listed in [Data S9](#).

Pyrosequencing

Pyrosequencing was performed to detect protein expression using a PyroMark Q96 instrument (Qiagen) as previously described.⁵⁸ The bisulfite-converted DNA was amplified using HotStarTaq DNA Polymerase (Qiagen). PCR products were immobilized on streptavidin-Sepharose beads (GE Healthcare, Chicago, IL), washed, denatured, and released into the annealing buffer containing sequencing primer ([Table S5](#)). Pyro CpG software (Qiagen) was used to calculate the percentage of methylation.

Statistical analysis

Normally distributed data are shown as mean \pm SEM and were compared using two-tailed Student's *t* test using GraphPad Prism

7.0 (www.graphpad.com). The number of independent experiments is shown in figure legends. A p value of less than 0.05 was considered to indicate statistical significance (*p < 0.05 and **p < 0.01; ns, not statistical significance).

SUPPLEMENTAL INFORMATION

Supplemental information can be found online at <https://doi.org/10.1016/j.ymthe.2022.01.043>.

ACKNOWLEDGMENTS

This project was supported by the National Natural Science Foundation of China (grant 82001578 to Y.X.; grant 81801472 to Y.Z.), the Project of Natural Science Foundation of Jiangsu Province (grant BK2020107 to Y.X.; grant BK20181080 to Y.Z.), the Postdoctoral Fund Project in Jiangsu Province (grant 2020Z087 to Y.X.), the Postdoctoral Fund Project in Nanjing (grant 2021BSH209 to Y.X.), Maternal and child health "young talents" project (grant FRC202151 to Y.X.), and the China Postdoctoral Fund Project (NO. 2020M671394 to Y.X.).

AUTHOR CONTRIBUTIONS

Y.X., Y.Z., and L. Sun designed and performed the experiments, collected and analyzed the data, and wrote the manuscript. Y.X., D.W., B.H., and L. Shu performed the experiments and collected and analyzed the data. N.Y., X.T., and C.W. performed the experiments and collected the data. Y.Z. provided intellectual insights and critical discussion of the project. Y.Y. and L. Shu created a heatmap showing the expression of differential genes after suppression of *TUG1*. All authors revised the manuscript critically for important intellectual content and read and approved the final version.

DECLARATION OF INTERESTS

The authors declare no competing interests.

REFERENCES

- American College of Obstetricians and Gynecologists (2013). Hypertension in pregnancy. Report of the American college of obstetricians and gynecologists' task force on hypertension in pregnancy. *Obstet. Gynecol.* 122, 1122–1131. <https://doi.org/10.1097/01.AOG.0000437382.03963.88>.
- Altman, D., Carroli, G., Duley, L., Farrell, B., Moodley, J., Neilson, J., Smith, D., and Magpie Trial Collaboration, G. (2002). Do women with pre-eclampsia, and their babies, benefit from magnesium sulphate? The Magpie Trial: a randomised placebo-controlled trial. *Lancet* 359, 1877–1890. [https://doi.org/10.1016/s0140-6736\(02\)08778-0](https://doi.org/10.1016/s0140-6736(02)08778-0).
- Hogberg, U. (2005). The World Health Report 2005: "make every mother and child count" - including Africans. *Scand. J. Public Health* 33, 409–411. <https://doi.org/10.1080/14034940500217037>.
- Genest, D.S., Falcao, S., Gutkowska, J., and Lavoie, J.L. (2012). Impact of exercise training on preeclampsia: potential preventive mechanisms. *Hypertension* 60, 1104–1109. <https://doi.org/10.1161/HYPERTENSIONAHA.112.194050>.
- Meekins, J.W., Pijnenborg, R., Hanssens, M., McFadyen, I.R., and van Asshe, A. (1994). A study of placental bed spiral arteries and trophoblast invasion in normal and severe pre-eclamptic pregnancies. *Br. J. Obstet. Gynaecol.* 101, 669–674. <https://doi.org/10.1111/j.1471-0528.1994.tb13182.x>.
- Pijnenborg, R., Vercruyse, L., and Hanssens, M. (2006). The uterine spiral arteries in human pregnancy: facts and controversies. *Placenta* 27, 939–958. <https://doi.org/10.1016/j.placenta.2005.12.006>.
- Soleymanlou, N., Jurisica, I., Nevo, O., Ietta, F., Zhang, X., Zamudio, S., Post, M., and Caniggia, I. (2005). Molecular evidence of placental hypoxia in preeclampsia. *J. Clin. Endocrinol. Metab.* 90, 4299–4308. <https://doi.org/10.1210/jc.2005-0078>.
- Maynard, S.E., Min, J.Y., Merchan, J., Lim, K.H., Li, J., Mondal, S., Libermann, T.A., Morgan, J.P., Sellke, F.W., Stillman, I.E., et al. (2003). Excess placental soluble fms-like tyrosine kinase 1 (sFlt1) may contribute to endothelial dysfunction, hypertension, and proteinuria in preeclampsia. *J. Clin. Invest.* 111, 649–658. <https://doi.org/10.1172/JCI17189>.
- Chaiworapongsa, T., Chaemsaitong, P., Yeo, L., and Romero, R. (2014). Preeclampsia part I: current understanding of its pathophysiology. *Nat. Rev. Nephrol.* 10, 466–480. <https://doi.org/10.1038/nrneph.2014.102>.
- Huppertz, B. (2008). Placental origins of preeclampsia: challenging the current hypothesis. *Hypertension* 51, 970–975. <https://doi.org/10.1161/HYPERTENSIONAHA.107.107607>.
- Sitras, V., Paulssen, R.H., Gronaas, H., Leirvik, J., Hanssen, T.A., Vartun, A., and Acharya, G. (2009). Differential placental gene expression in severe preeclampsia. *Placenta* 30, 424–433. <https://doi.org/10.1016/j.placenta.2009.01.012>.
- Guttman, M., Amit, I., Garber, M., French, C., Lin, M.F., Feldser, D., Huarte, M., Zuk, O., Carey, B.W., Cassady, J.P., et al. (2009). Chromatin signature reveals over a thousand highly conserved large non-coding RNAs in mammals. *Nature* 458, 223–227. <https://doi.org/10.1038/nature07672>.
- Charles Richard, J.L., and Eichhorn, P.J.A. (2018). Platforms for investigating lncRNA functions. *SLAS Technol.* 23, 493–506. <https://doi.org/10.1177/2472630318780639>.
- Lan, W., Li, M., Zhao, K., Liu, J., Wu, F.X., Pan, Y., and Wang, J. (2017). LDAP: a web server for lncRNA-disease association prediction. *Bioinformatics* 33, 458–460. <https://doi.org/10.1093/bioinformatics/btw639>.
- Kopp, F., and Mendell, J.T. (2018). Functional classification and experimental dissection of long noncoding RNAs. *Cell* 172, 393–407. <https://doi.org/10.1016/j.cell.2018.01.011>.
- Akerman, I., Tu, Z., Beucher, A., Rolando, D.M.Y., Sauty-Colace, C., Benazra, M., Nakić, N., Yang, J., Wang, H., Pasquali, L., et al. (2017). Human pancreatic beta cell lncRNAs control cell-specific regulatory networks. *Cell Metab.* 25, 400–411. <https://doi.org/10.1016/j.cmet.2016.11.016>.
- Schmitz, S.U., Grote, P., and Herrmann, B.G. (2016). Mechanisms of long noncoding RNA function in development and disease. *Cell Mol. Life Sci.* 73, 2491–2509. <https://doi.org/10.1007/s00018-016-2174-5>.
- Liao, K., Xu, J., Yang, W., You, X., Zhong, Q., and Wang, X. (2018). The research progress of lncRNA involved in the regulation of inflammatory diseases. *Mol. Immunol.* 101, 182–188. <https://doi.org/10.1016/j.molimm.2018.05.030>.
- Ghazal, S., McKinnon, B., Zhou, J., Mueller, M., Men, Y., Yang, L., Mueller, M., Flannery, C., Huang, Y., and Taylor, H.S. (2015). H19 lncRNA alters stromal cell growth via IGF signaling in the endometrium of women with endometriosis. *EMBO Mol. Med.* 7, 996–1003. <https://doi.org/10.15252/emmm.201505245>.
- Akhade, V.S., Pal, D., and Kanduri, C. (2017). Long noncoding RNA: genome organization and mechanism of action. *Adv. Exp. Med. Biol.* 1008, 47–74. https://doi.org/10.1007/978-981-10-5203-3_2.
- Xu, Y., Wu, D., Liu, J., Huang, S., Zuo, Q., Xia, X., Jiang, Y., Wang, S., Chen, Y., Wang, T., and Sun, L. (2018). Downregulated lncRNA HOXA11-AS affects trophoblast cell proliferation and migration by regulating RND3 and HOXA7 expression in PE. *Mol. Ther. Nucleic Acids* 12, 195–206. <https://doi.org/10.1016/j.omtn.2018.05.007>.
- Lin, P.C., Huang, H.D., Chang, C.C., Chang, Y.S., Yen, J.C., Lee, C.C., Chang, W.H., Liu, T.C., and Chang, J.G. (2016). Long noncoding RNA TUG1 is downregulated in non-small cell lung cancer and can regulate CELF1 on binding to PRC2. *BMC Cancer* 16, 583. <https://doi.org/10.1186/s12885-016-2569-6>.
- Li, Q., Zhang, J., Su, D.M., Guan, L.N., Mu, W.H., Yu, M., Ma, X., and Yang, R.J. (2019). lncRNA TUG1 modulates proliferation, apoptosis, invasion, and angiogenesis via targeting miR-29b in trophoblast cells. *Hum. Genomics* 13, 50. <https://doi.org/10.1186/s40246-019-0237-z>.
- Ai, Y., Chen, M., Liu, J., Ren, L., Yan, X., and Feng, Y. (2020). lncRNA TUG1 promotes endometrial fibrosis and inflammation by sponging miR-590-5p to regulate FasI in intrauterine adhesions. *Int. Immunopharmacol.* 86, 106703. <https://doi.org/10.1016/j.intimp.2020.106703>.

25. Xu, Y., Ge, Z., Zhang, E., Zuo, Q., Huang, S., Yang, N., Wu, D., Zhang, Y., Chen, Y., Xu, H., et al. (2017). The lncRNA TUG1 modulates proliferation in trophoblast cells via epigenetic suppression of RND3. *Cell Death Dis.* 8, e3104. <https://doi.org/10.1038/cddis.2017.503>.
26. Wu, A.H., Yang, D.Y., Liu, Y.D., Chen, X., Chen, X.L., Lu, S., and Chen, S.L. (2018). Expression of TET and 5-HmC in trophoblast villi of women with normal pregnancy and with early pregnancy loss. *Curr. Med. Sci.* 38, 505–512. <https://doi.org/10.1007/s11596-018-1907-0>.
27. Muramatsu, D., Kimura, H., Kotoshiba, K., Tachibana, M., and Shinkai, Y. (2016). Pericentric H3K9me3 formation by HP1 interaction-defective histone methyltransferase Suv39h1. *Cell Struct. Funct.* 41, 145–152. <https://doi.org/10.1247/csf.16013>.
28. An, J., Rao, A., and Ko, M. (2017). TET family dioxygenases and DNA demethylation in stem cells and cancers. *Exp. Mol. Med.* 49, e323. <https://doi.org/10.1038/emmm.2017.5>.
29. Rasmussen, K.D., and Helin, K. (2016). Role of TET enzymes in DNA methylation, development, and cancer. *Genes Dev.* 30, 733–750. <https://doi.org/10.1101/gad.276568.115>.
30. Minor, E.A., Court, B.L., Young, J.L., and Wang, G. (2013). Ascorbate induces ten-eleven translocation (Tet) methylcytosine dioxygenase-mediated generation of 5-hydroxymethylcytosine. *J. Biol. Chem.* 288, 13669–13674. <https://doi.org/10.1074/jbc.C113.464800>.
31. Ma, M., Zhou, Q.J., Xiong, Y., Li, B., and Li, X.T. (2018). Preeclampsia is associated with hypermethylation of IGF-1 promoter mediated by DNMT1. *Am. J. Transl. Res.* 10, 16–39.
32. Cao, T., Jiang, Y., Wang, Z., Zhang, N., Al-Hendy, A., Mamillapalli, R., Kallen, A.N., Kodaman, P., Taylor, H.S., Li, D., and Huang, Y. (2019). H19 lncRNA identified as a master regulator of genes that drive uterine leiomyomas. *Oncogene* 38, 5356–5366. <https://doi.org/10.1038/s41388-019-0808-4>.
33. Cheng, S.B., Nakashima, A., Huber, W.J., Davis, S., Banerjee, S., Huang, Z., Saito, S., Sadovsky, Y., and Sharma, S. (2019). Pyroptosis is a critical inflammatory pathway in the placenta from early onset preeclampsia and in human trophoblasts exposed to hypoxia and endoplasmic reticulum stressors. *Cell Death Dis.* 10, 927. <https://doi.org/10.1038/s41419-019-2162-4>.
34. Fang, M., Du, H., Han, B., Xia, G., Shi, X., Zhang, F., Fu, Q., and Zhang, T. (2017). Hypoxia-inducible microRNA-218 inhibits trophoblast invasion by targeting LASP1: implications for preeclampsia development. *Int. J. Biochem. Cell Biol.* 87, 95–103. <https://doi.org/10.1016/j.biocel.2017.04.005>.
35. Mol, B.W.J., Roberts, C.T., Thangaratnam, S., Magee, L.A., de Groot, C.J.M., and Hofmeyr, G.J. (2016). Pre-eclampsia. *Lancet* 387, 999–1011. [https://doi.org/10.1016/S0140-6736\(15\)00070-7](https://doi.org/10.1016/S0140-6736(15)00070-7).
36. Phipps, E.A., Thadhani, R., Benzing, T., and Karumanchi, S.A. (2019). Pre-eclampsia: pathogenesis, novel diagnostics and therapies. *Nat. Rev. Nephrol.* 15, 275–289. <https://doi.org/10.1038/s41581-019-0119-6>.
37. Winkle, M., El-Daly, S.M., Fabbri, M., and Calin, G.A. (2021). Noncoding RNA therapeutics - challenges and potential solutions. *Nat. Rev. Drug Discov.* 20. <https://doi.org/10.1038/s41573-021-00219-z>.
38. Qian, X., Zhao, J., Yeung, P.Y., Zhang, Q.C., and Kwok, C.K. (2019). Revealing lncRNA structures and interactions by sequencing-based approaches. *Trends Biochem. Sci.* 44, 33–52. <https://doi.org/10.1016/j.tibs.2018.09.012>.
39. Schertz, M.D., Braceros, K.C.A., Starmer, J., Cherney, R.E., Lee, D.M., Salazar, G., Justice, M., Bischoff, S.R., Cowley, D.O., Ariel, P., et al. (2019). lncRNA-induced spread of polycomb controlled by genome architecture, RNA abundance, and CpG island DNA. *Mol. Cell* 75, 523–537.e10. <https://doi.org/10.1016/j.molcel.2019.05.028>.
40. Brook, I., and Yocum, P. (1988). Comparison of the microbiology of group A and non-group A streptococcal tonsillitis. *Ann. Otol. Rhinol. Laryngol.* 97, 243–246. <https://doi.org/10.1177/000348948809700306>.
41. Tsgaratou, A. (2021). Deciphering the multifaceted roles of TET proteins in T-cell lineage specification and malignant transformation. *Immunol. Rev.* 300, 22–36. <https://doi.org/10.1111/imr.12940>.
42. Ramkissoon, A., Chaney, K.E., Milewski, D., Williams, K.B., Williams, R.L., Choi, K., Miller, A., Kalin, T.V., Pressey, J.G., Szabo, S., et al. (2019). Targeted inhibition of the dual specificity phosphatases DUSP1 and DUSP6 suppress MPNST growth via JNK. *Clin. Cancer Res.* 25, 4117–4127. <https://doi.org/10.1158/1078-0432.CCR-18-3224>.
43. Jimenez, T., Barrios, A., Tucker, A., Collazo, J., Arias, N., Fazel, S., Baker, M., Halim, M., Huynh, T., Singh, R., and Pervin, S. (2020). DUSP9-mediated reduction of pERK1/2 supports cancer stem cell-like traits and promotes triple negative breast cancer. *Am. J. Cancer Res.* 10, 3487–3506.
44. Guo, C.J., Ma, X.K., Xing, Y.H., Zheng, C.C., Xu, Y.F., Shan, L., Zhang, J., Wang, S., Wang, Y., Carmichael, G.G., et al. (2020). Distinct processing of lncRNAs contributes to non-conserved functions in stem cells. *Cell* 181, 621–636.e2. <https://doi.org/10.1016/j.cell.2020.03.006>.
45. Matsui, H., Iriyama, T., Sayama, S., Inaoka, N., Suzuki, K., Yoshikawa, M., Ichinose, M., Sone, K., Kumasawa, K., Nagamatsu, T., et al. (2021). Elevated placental histone H3K4 methylation via upregulated histone methyltransferases SETD1A and SMYD3 in preeclampsia and its possible involvement in hypoxia-induced pathophysiological process. *Placenta* 115, 60–69. <https://doi.org/10.1016/j.placenta.2021.09.009>.
46. Kazmi, N., Sharp, G.C., Reese, S.E., Vehmeijer, F.O., Lahti, J., Page, C.M., Zhang, W., Rifas-Shiman, S.L., Rezwan, F.I., Simpkin, A.J., et al. (2019). Hypertensive disorders of pregnancy and DNA methylation in newborns. *Hypertension* 74, 375–383. <https://doi.org/10.1161/HYPERTENSIONAHA.119.12634>.
47. Apicella, C., Ruano, C.S.M., Mehats, C., Miralles, F., and Vaiman, D. (2019). The role of epigenetics in placental development and the etiology of preeclampsia. *Int. J. Mol. Sci.* 20. <https://doi.org/10.3390/ijms20112837>.
48. Shen, J.Z., Qiu, Z., Wu, Q., Finlay, D., Garcia, G., Sun, D., Rantala, J., Barshop, W., Hope, J.L., Gimple, R.C., et al. (2021). FBXO44 promotes DNA replication-coupled repetitive element silencing in cancer cells. *Cell* 184, 352–369.e3. <https://doi.org/10.1016/j.cell.2020.11.042>.
49. Zhuang, T., Liu, J., Chen, X., Zhang, L., Pi, J., Sun, H., Li, L., Bauer, R., Wang, H., Yu, Z., et al. (2019). Endothelial Foxp1 suppresses atherosclerosis via modulation of Nlrp3 inflammasome activation. *Circ. Res.* 125, 590–605. <https://doi.org/10.1161/CIRCRESAHA.118.314402>.
50. Frazier, S., McBride, M.W., Mulvana, H., and Graham, D. (2020). From animal models to patients: the role of placental microRNAs, miR-210, miR-126, and miR-148a/152 in preeclampsia. *Clin. Sci. (Lond)* 134, 1001–1025. <https://doi.org/10.1042/CS20200023>.
51. Brkic, J., Dunk, C., O'Brien, J., Fu, G., Nadeem, L., Wang, Y.L., Rosman, D., Salem, M., Shynlova, O., Yougbare, I., et al. (2018). MicroRNA-218-5p promotes endovascular trophoblast differentiation and spiral artery remodeling. *Mol. Ther.* 26, 2189–2205. <https://doi.org/10.1016/j.yjthe.2018.07.009>.
52. Thomson, D.W., and Dinger, M.E. (2016). Endogenous microRNA sponges: evidence and controversy. *Nat. Rev. Genet.* 17, 272–283. <https://doi.org/10.1038/nrg.2016.20>.
53. Kumar, V., Kumar, V., Chaudhary, A.K., Coulter, D.W., McGuire, T., and Mahato, R.I. (2018). Impact of miRNA-mRNA profiling and their correlation on medulloblastoma tumorigenesis. *Mol. Ther. Nucleic Acids* 12, 490–503. <https://doi.org/10.1016/j.omtn.2018.06.004>.
54. Zhang, S., Zou, Y., Tang, X., Zhang, Y., Yang, N., Xu, K., and Xu, Y. (2021). Silencing of AFAP1-AS1 lncRNA impairs cell proliferation and migration by epigenetically promoting DUSP5 expression in pre-eclampsia. *J. Cell Biochem.* 122. <https://doi.org/10.1002/jcb.30072>.
55. Geng, T., Liu, Y., Xu, Y., Jiang, Y., Zhang, N., Wang, Z., Carmichael, G.G., Taylor, H.S., Li, D., and Huang, Y. (2018). H19 lncRNA promotes skeletal muscle insulin sensitivity in part by targeting AMPK. *Diabetes* 67, 2183–2198. <https://doi.org/10.2337/db18-0370>.
56. Xu, Y., Sun, X., Zhang, R., Cao, T., Cai, S.Y., Boyer, J.L., Zhang, X., Li, D., and Huang, Y. (2020). A positive feedback loop of TET3 and TGF-beta1 promotes liver fibrosis. *Cell Rep.* 30, 1310–1318.e5. <https://doi.org/10.1016/j.celrep.2019.12.092>.
57. Zhang, E., Han, L., Yin, D., He, X., Hong, L., Si, X., Qiu, M., Xu, T., De, W., Xu, L., et al. (2017). H3K27 acetylation activated-long non-coding RNA CCAT1 affects cell proliferation and migration by regulating SPRY4 and HOXB13 expression in esophageal squamous cell carcinoma. *Nucleic Acids Res.* 45, 3086–3101. <https://doi.org/10.1093/nar/gkw1247>.
58. Yu, Y.C., Jiang, Y., Yang, M.M., He, S.N., Xi, X., Xu, Y.T., Hu, W.S., and Luo, Q. (2019). Hypermethylation of delta-like homolog 1/maternally expressed gene 3 loci in human umbilical veins: insights into offspring vascular dysfunction born after preeclampsia. *J. Hypertens.* 37, 581–589. <https://doi.org/10.1097/HJH.0000000000001942>.

YMTHE, Volume 30

Supplemental Information

**A novel regulatory mechanism network mediated
by lncRNA *TUG1* that induces the impairment
of spiral artery remodeling in preeclampsia**

Yetao Xu, Dan Wu, Bingqing Hui, Lijun Shu, Xiaotong Tang, Cong Wang, Jiaheng Xie, Yin Yin, Matthew Sagnelli, Nana Yang, Ziyang Jiang, Yuanyuan Zhang, and Lizhou Sun

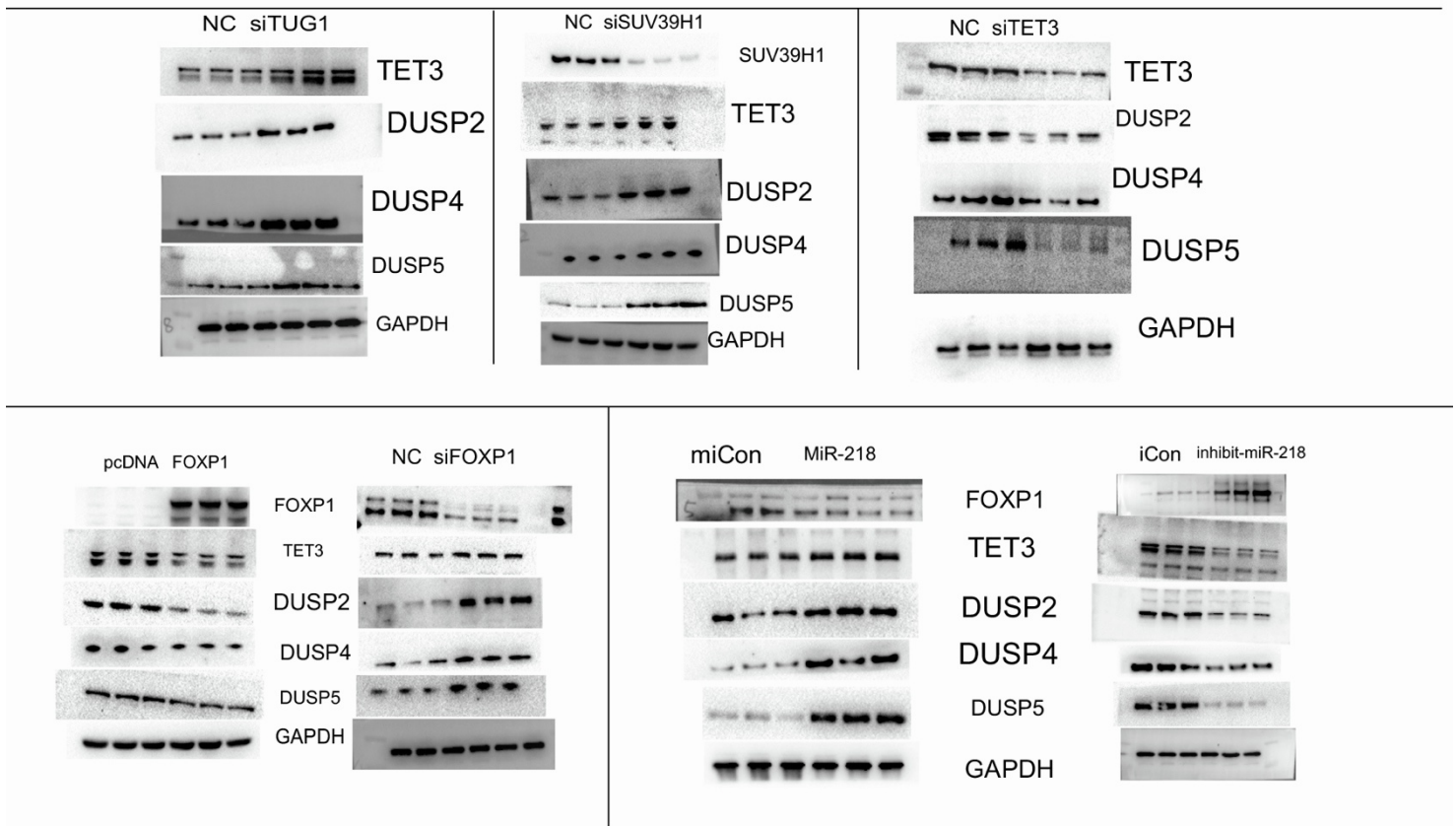
Supplementary file 1 : The list of PCR / CHIP-PCR primers and siRNAs sequences

Real-time PCR primer sequences (human)		
Gene	Forward Primer	Reverse Primer
GAPDH	5' - CTTTGTCAAGCTCATTTCCTGG -3'	5' - TCTTCCTCTTGTGCTCTTGC -3'
ACTB	5' - ATCAAGATCATTGCTCCTCCTGAG-3'	5' - CTGCTTGCTGATCCACATCTG-3'
TET1	5' - GCAGCGTACAGGCCACCACT -3'	5' - AGCCGGTCGGCCATTGGAAG -3'
TET2	5' - TTCGCAGAAGCAGCAGTGAAGAG-3'	5' - AGCCAGAGACAGCGGGATTCCCTT-3'
TET3	5' -GACGAGAACATCGGCGGCGT -3'	5' - GTGGCAGCGTTGGGCTTCT-3'
TUG1	5' -TAGCAGTTCCCAATCCTTG -3'	5' -CACAAATTCATCATTCCC -3'
DUSP1	5' - AGTACCCCACTCTACGATCAGG -3'	5' - GAAGCGTGATACGCACTGC -3'
DUSP2	5' - TACTTCTCGGAGGAGGCTT -3'	5' - TAGACAGGAGCCCTGGAGTC -3'
DUSP4	5' - AGTGAAGATAACCACAAGG -3'	5' - GCTTAACGAACTCGAAGG -3'
DUSP5	5' -TGTCGTCCTCACCTCGCTA -3'	5' - GGGCTCTCTCACTCTCAATCTC -3'
DUSP6	5' - GATCACTGGAGCCAAAAC -3'	5' - CAAGCAATGTACCAAGACAC -3'
DUSP7	5' -CCAAGAAGTGTGGTGTCTCG -3'	5' -ACAAAGTCGTAGGCGTCGTT-3'
DUSP9	5' - CAGCCGTTCTGTCACCGTC -3'	5' - CAAGCTGCGCTCAAAGTCC -3'
DUSP10	5' - TTTGAAGAGGCTTTTGTGAGTT -3'	5' - GGGAGATAATTGGTCGTTT -3'
DUSP12	5' - gcagccaggattgtatttcg-3'	5' - agtaggtccgtctcgggttt -3'
DUSP13	5' - ATCTTGCCCTTCTGTTCTT-3'	5' - CTCCCACACTGGTGAGCTT-3'
FOXP1	5' - GTTGCACTCTGTGGCATT-3'	5' - TGACCGCCGCACTCTAGTAA -3'
CHIP-PCR primer sequences (human)		
TUG1 CHIP primer-1	5'-CATGAACACTGTATGTTTCTGTGGA-3'	5'-CTGGCAGATTGCTCACATCC-3'
TET3 CHIP primer-1	5'-AGCCTCCTTATTTTCGCACCC-3'	5'-TTGCTAGAGGAGGAAGCCCT-3'
TET3 CHIP primer-2	5'-CTGAGCGCAATGTGAATGGG-3'	5'-GCGCCCAAGATAAAAACAGCC-3'
TET3 CHIP primer-3	5'-CTCACCAATGCAGGTCCACA-3'	5'-ACACTGTTGGATGCTGCTGA-3'
DUSP2 CHIP primer-1	5'- TGACACCACTCCCCATCTC-3'	5'- CAGCACCTGGGTCTCAAAC-3'
DUSP2 CHIP primer-2	5' - GTATGTCCCGGTGTGTCCTC-3'	5'- ACCCAGTCTGCAAGGGAGAT-3'
DUSP4 CHIP primer-1	5' - GTCCCTTCTTAGCTCTCGCC-3'	5'- CATCTCCCGACTCCAGCTA-3'
DUSP4 CHIP primer-2	5'- GGCGTCCCTTCTTAGCTCTC-3'	5'- GACTCCTTCCCGTGCCAATA-3'
DUSP5 CHIP primer-1	5'- CCGGCCAAAGACTAAGACCC-3'	5'- GCGTACTGGAGGTATGTGGG-3'
DUSP5 CHIP primer-2	5'- CGCGGAAGAGAGAACGAAGA-3'	5'- ATGTGAATGAGTGCCGTCCG-3'
U6	5' - CTCGCTTCGGCAGCACA -3'	5' - AACGCTTACGAATTTGCGT -3'
Ago2	5' - CCCGCATCATCTTCTACCGC -3'	5' - GCTTGTCCTCCGCTCGTT -3'
hsa-miR-218-5p inhibitor (human)		
sense 5' - UUGUGCUUGAUCUAACCAUGU -3'		
antisense 5' - ACAUGGUUAGAUAAGCACAA -3'		
TUG1 siRNA sequence (human)		
1# sense 5' -UAGAAUUGUUCUCUGGCUAUAUCCC-3' , antisense 5' - GGGAUUAAGCCAGAGAACAAUUCUA-3'		
2# sense 5' -GCUUGGCUUCUAUUCUGAAUCCUUU-3' ,		

antisense 5' - AAAGGAUUCAGAAUAGAAGCCAAGC-3'
3# sense 5' -CAGCUGUUACCAUUCAACUUCUAAA-3' , antisense 5' -UUAAGAAGUUGAAUGGUAACAGCUG-3'
TET3 siRNA sequence (human)
1# sense 5' -CAGCAACUCCUAGAACUGAtt-3' , antisense 5' - UCAGUUCUAGGAGUUGCUGga -3'
2# sense 5' - CGAUUGCGUCGAACAAAUAtt-3' , antisense 5' - UAUUUGUUCGACGCAAUCGca -3'
TET1 siRNA sequence (human)
1# sense 5' - CCCAAGUCAUGCAGCCCUAtt-3' , antisense 5' -UAGGGCUGCAUGACUUGGGcg -3'
2# sense 5' - GCUAUACGCUAAAUUACCAAtt -3' , antisense 5' -UGGUAAUUAAGCGUAUAGCat -3'
TET2 siRNA sequence (human)
1# sense 5' - CCCAAUCUCUCCAAUCAAAAtt-3' , antisense 5' - UUUGAUUGGAGAGAUUGGGtt
2# sense 5' - GAGUUGUCCUGUGAGAUCAtt-3' , antisense 5' -UGAUCUCACAGGACAACUCat -3'
SAHH siRNA sequence (human)
1# sense 5' - CAAGCUAACUGAGAAGCAAtt-3' , antisense 5' - UUGCUUCUCAGUUAGCUUGgt -3'
FXOP1 siRNA sequence (human)
1# sense 5' - CTCAGTCCACACTCCCAAA -3'
2# sense 5' - CCACAGAGCTTACCTCATA -3'
3# sense 5' - CTGGTTCACACGAATGTTT -3'
SUV39H1 siRNA sequence (human)
1# sense 5' - GCATCACTGTAGAGAATGA -3'
2# sense 5' - GGGTCCGTATTGAATGCAA -3'
3# sense 5' - GGGCCTTCGTGTACATCAA -3'

Supplemental file 2: Uncut western gel images.

Uncut Western gel images



Supplemental file 3: The binding sites of TUG1 with FOXP1.

TUG1 promoter region (2000bp)

Binding to FOXP1 Prediction

>NC_000022.11:30967211-30969211 Homo sapiens chromosome 22, GRCh38.p12 Primary Assembly

(-2000)
 AGAACCATGAACACTGTATGTTTCTGTGGAAATTTGGGGAAAGACTATCTAAATA (-
 1943) GAGATATAACAAGT (-1929)
 TGTGCCGTTTCCTGTTTAGCATATACAATAATATTGGAT
 GTGAGCAATCTGCCAGGAAGATAATGCCAACTTCTGAAAAATAAAAAATTTCTTCTTGAA
 AGTTGTCATTTAAATGTCTTCTGTTTTCTTGTT (-1796) AGAAAGTAAACACTT (-1782)
 GTTATAAACCTAACTGTTTAGGACGTTGTCACTACAGAGGGGAAACGGTTGATACTAAA

ATAGTCCAACATTTGGCGATCCAATAGAGCAGTATTTGTTGGATTCTATAAACACTTGAA
TGAAACAACACTCAACATATTGACTTCAAATAACTAAAGTTTGCATTTAGAAAATTTG (-
1604) ATCCAATAAACAAAA (-1590) ATCAGTGATCTCAGTTCTTCAATACAGAGCT
CAAGATATCCAGTGACACATTTCACTCCAGTGGGATACATCTCAAAAAGTGAAAAAGCAA
AATTTTCTGGGGAAACGATTTCCATATAATATCAAGGAACGAGTACTGGTTACCTCAGT
GGCACCTAGAGGATACTTACGAATTTGTGTGCAGATATTCAAAGGTTAGCTGAGCTCGAT
TCAGACTGCTGTAATTTGTGAAAGCCATGACTGCAATAAGGTCTCCAGCCCTTCACCCG
CTAACTGGGAAATATAACCTTATAATGATATCGATTTCCAGGATTCTGTCCAGTAAAGCT
TCAGTAAGTCTGTGCTCCTTAATGACAGTTAAAGTAACCTAGTAGCTATCCAAAATATATG
CAGAGATGTTTAAACTACAATTTCTTCAAGTGTTTTTTTTTAATCTTCTCAATGATTTATG
ATGTAATATTTTGAAGGAACTATGTCATAAATCTGTAGCTTTAAGGAGCTTTTAGCATT
AGTTGCGATAGCTCAATTCAGACAATCTGAGTCTCGTGTGGATGGTCCTGAAGGAGATG
GTCCTTGAGTGGGTGGTTTATGACTGCTCCATCTTCATGTTCTTCCAGCCTTTTTTGGTTC
CCCGAAATTTCTGTGAGGAAATTTACCAACGCGGAAATTTACCCACTTCTGTGAGAAA
CTGATCAGCCATGTCTTCGCCACACGTGATGCCAGGATTCTTAAACAGGCCCAAGACCG
GAGACCAAGATGTCGACGGAGTGTTATATGGCGCAAGTTGCAGCTTACCACCTCCCAA
GTGAAAAAGCTCCTAGGCACTCACGATTTCTTTTTTCAAAGCCGGACCAAACCCAGTTCA
GGGTGGTGGTCAGATTACCTCACACTTGGCCACATAAACACCTCACAAATGACCCGCC
CACAGCACCTCGGGCAGGCCGCGCCCCGCCCCACGTCCCTCAGACAACAGCCTCAG
CCTCCCAGGCCCTTCCCGGGCCTCGGTCCCGTGGCCGCCTCCCACGAAGAGGAGCTA
CTCCCGGCTTCCAAGGACCGGATCGAGGGCAGTGGCGAGCGCACCACTGACCGGGC
ACTACCCGGATCTCACAACACTGCCTTTGTCCCTCCCCGCGGAATTGGAACCCAACAGCCG
CAGAGCGCTCTTGAACCATGTGCTGCTGCCGCCTCCGCCGCCGCCGCCGCTGCCTCC
GCCGCCGCCGCCGCCGCCGCCGCCGCCGCCGCTAGTTGAGATGGTGACAGGATTAG
CAACACGAAATTCGGCGTTTGTAGAGCTGCTCTGCCGCCGCCGTCACAGACACCACAGCC
ACCGCTTTGTCTCCGATAGTGACACAGCCCCGGCCACCTCGCACACTCCCCGACGCC
CCAAGCCCCCGAGGCCTCCGCGGAGCATTAGCCAATCACAAGCTGCAGCTCCTCCC
GCCCCGCCCTGATGTACAGCCTCCTGATTGGCGGGCTGCGTGTCCCATGTGACCGG
ATCTTGGTTGGCCGGTCCCGCCCCTGTCACGTGACAGCGTGCGCCTCTCTT (-1)

Yellow: The position of the representative locus in the promoter region.

Red: The corresponding base sequence site.

6 putative sites were predicted with these settings (80%) in sequence named **NC_000022.11:30967211-30969211**

Model ID	Model name	Score	Relative score	Start	End	Strand	predicted site sequence
MA0481.1	FOXP1	10.085	0.836492339754999	57	71	1	GAGATATAACAAGT
MA0481.1	FOXP1	14.567	0.909936734368791	189	203	-1	AACAAGAAAACAGAA
MA0481.1	FOXP1	13.030	0.884750649022651	204	218	1	AGAAAGTAAACACTT
MA0481.1	FOXP1	13.467	0.891911559430109	396	410	1	ATCCAATAAACAAAA
MA0481.1	FOXP1	10.182	0.838081832454137	861	875	-1	TAAAAAAAAAACTT
MA0481.1	FOXP1	8.556	0.811437346590232	863	877	-1	ATTAAAAAAAAAACAC

Comment: This type of analysis has a high sensitivity but abysmal selectivity. In other words: while true functional will be detected in most cases, most predictions will correspond to sites bound in vitro but with no function in vivo. A number of additional constraints of the analysis can improve the prediction; phylogenetic footprinting is the most common. We recommend using the [ConSite](#) service, which uses the JASPAR datasets.

The review [Nat Rev Genet. 2004 Apr;5\(4\):276-87](#) gives a comprehensive overview of transcription binding site prediction

Supplemental file 4: Detailed process of methyltarget sequencing.

Acknowledgement

We acknowledged the technical support from the Shanghai Genesky Biotechnology Company (Shanghai, China).

Detailed process of methyltarget sequencing.

CpG islands selected

CpG islands located in the proximal promoter of DUSP2, DUSP4 and DUSP5 were selected for measurement according to the following criteria: (1) 200 bp minimum length; (2) 50% or higher GC content; (3) 0.60 or higher ratio of observed/expected dinucleotides CpG.

Bisulfite conversion and multiplex amplification

DNA methylation level was analysis by MethylTarget® (Genesky Biotechnologies Inc., Shanghai, China), an NGS-based multiple Targeted CpG methylation analysis method. Specifically, the genomic regions of interest were analyzed and transformed to bisulfite-converted sequences by geneCpG software. PCR primer sets were designed with the Methylation Primer software from bisulfate converted DNA.

Genomic DNA (400ng) was subjected to sodium bisulfite treatment using EZ DNA Methylation™-GOLD Kit (Zymo Research) according to manufacturer's protocols. Multiplex PCR was performed with optimized primer sets combination. A 20 µl PCR reaction mixture was prepared for each reaction and included 1x reaction buffer (Takara), 3 mM Mg²⁺, 0.2 mM dNTP, 0.1 µM of each primer, 1U HotStarTaq polymerase (Takara) and 2 µl template DNA. The cycling program was 95°C for 2 min; 11 cycles of 94°C for 20 s, 63°C for 40s with a decreasing temperature step of 0.5°C per cycle, 72°C for 1 min; then followed by 24 cycles of 94°C for 20 s, 65°C for 30 s, 72°C for 1 min; 72°C for 2 min.

Index PCR

PCR amplicons were diluted and amplified using indexed primers. Specifically, a 20 µl mixture was prepared for each reaction and included 1x reaction buffer (NEB Q5™), 0.3 mM dNTP, 0.3 µM of F primer, 0.3 µM of index primer, 1 U Q5™ DNA polymerase (NEB) and 1 µL diluted template. The cycling program was 98°C for 30 s; 11 cycles of 98°C for 10 s, 65°C for 30 s, 72°C for 30 s; 72°C for 5 min. PCR amplicons (170bp-270bp) were separated by agarose electrophoresis and purified using QIAquick Gel Extraction kit (QIAGEN).

Sequencing

Libraries from different samples were quantified and pooled together, followed by sequencing on the Illumina MiSeq platform according to manufacturer's protocols. Sequencing was performed with a 2x150bp paired-end mode.

Data analysis

FLASH (Fast Length Adjustment of SHort reads) is an accurate and fast tool, which was used to merge paired-end reads[1]. Fastq to fasta format step was then processed using the Fastx toolkit (http://hannonlab.cshl.edu/fastx_toolkit/index.html). Reads with fasta format were mapped to targeted Bisulfite Genome (hg19) by Blast [2]. Unmapped reads were filtered and mapped reads with coverage greater than 90% and identity greater than 95% were kept as effective reads and were used for following statistics. Sequencing depth for each amplicon per sample was calculated by blasting the effective reads against the targeted genome region. Reads less than 10-fold were removed and overall sequencing depth for each sample were evaluated. Methylation and haplotype were analyzed using Perl script. Statistics were performed by t-test and ANOVA.

1 Magoc T , Salzberg S L . FLASH: fast length adjustment of short reads to improve genome assemblies[J]. Bioinformatics, 2011, 27(21):2957-2963.

2 Camacho C , Coulouris G , Avagyan V , et al. BLAST+: architecture and applications[J]. BMC

Bioinformatics, 2009, 10(1):421-0.

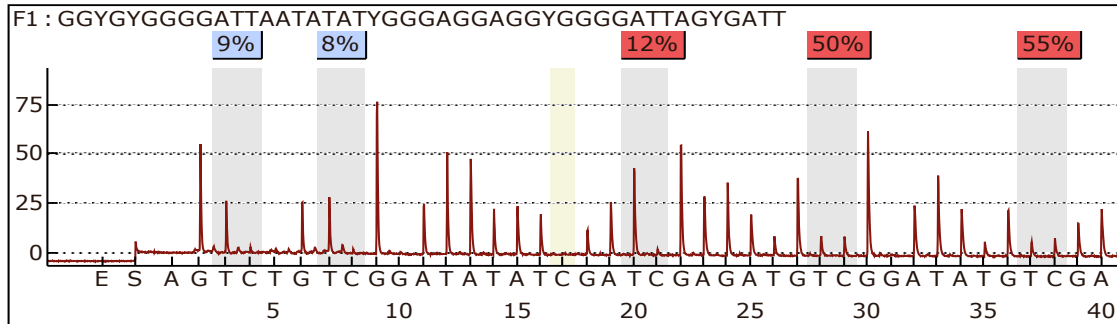
Supplemental file 5: Promoter demethylation levels of DUSP2, DUSP4 and DUSP5 genes detected by pyrosequencing.

DUSP2

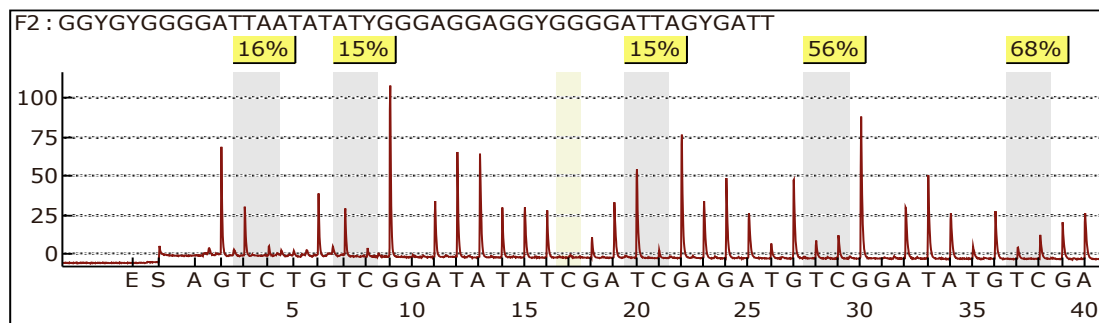
Assay Name: PM403-1FS

Sample ID: 1-1

siCon



siTET3

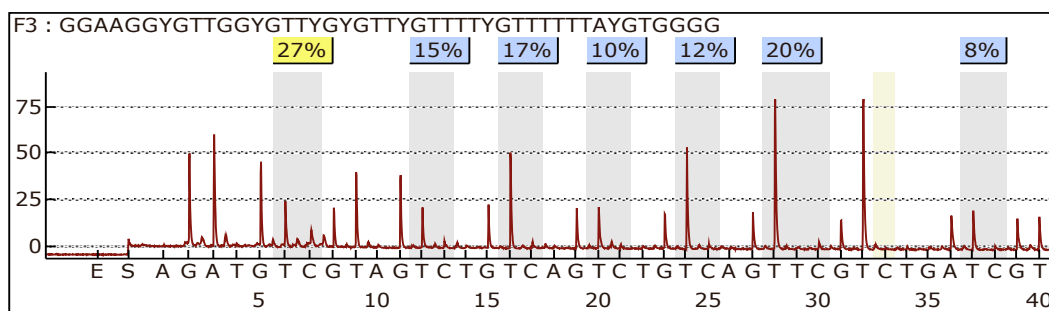


DUSP2

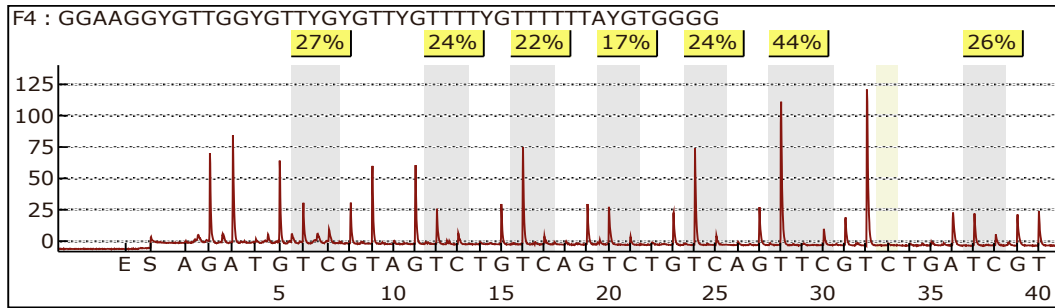
Assay Name: PM403-2FS

Sample ID: 2-1

siCon



siTET3

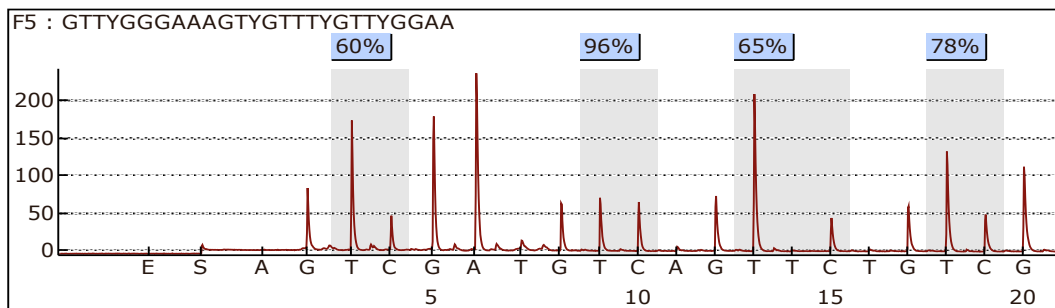


DUSP4

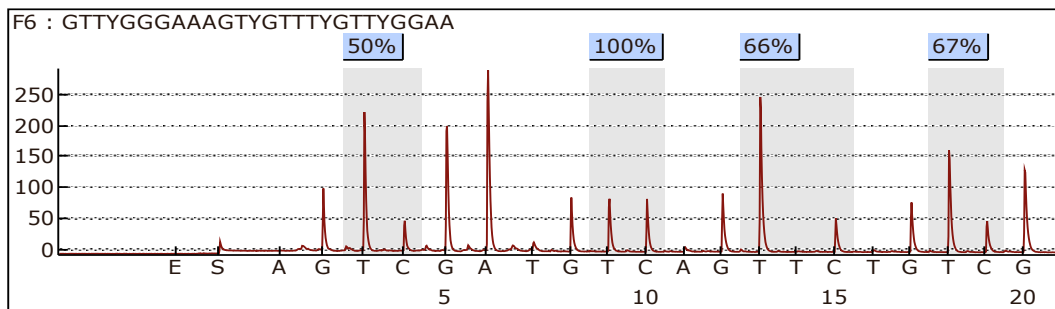
Assay Name: PM43-3FS

Sample ID: 3-1

siCon



siTET3

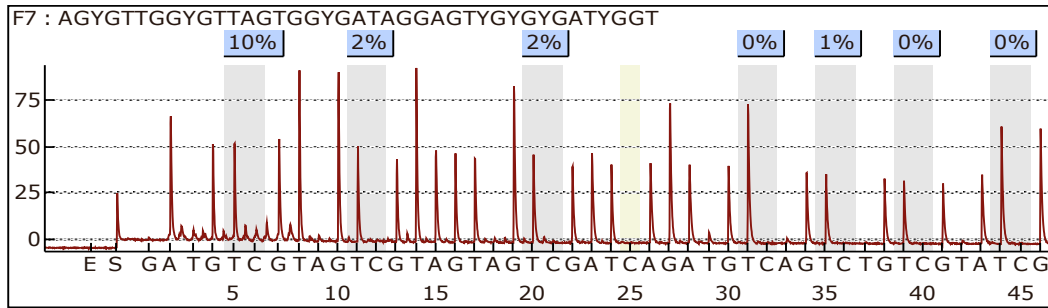


DUSP4

Assay Name: PM403-4FS

Sample ID: 4-1

siCon



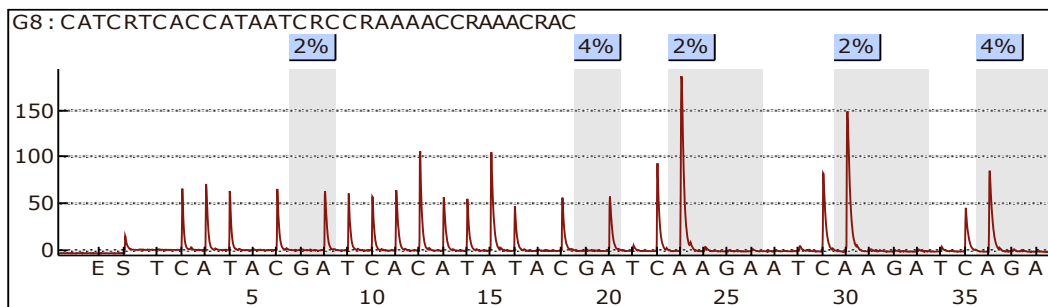
siTET3

DUSP4

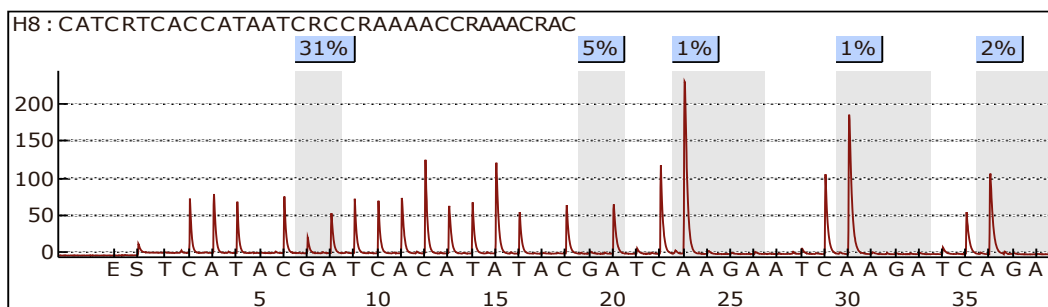
Assay Name: PM403-5FS

Sample ID: 1

siCon



siTET3

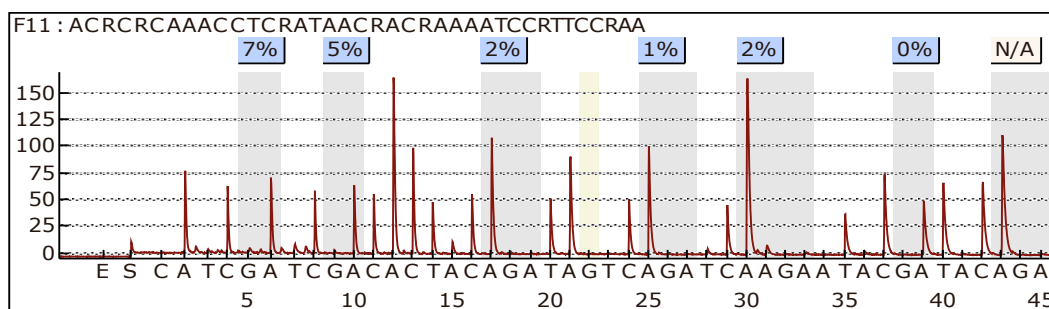


DUSP5

Assay Name: PM403-6RS

Sample ID: 6-1

siCon



siTET3

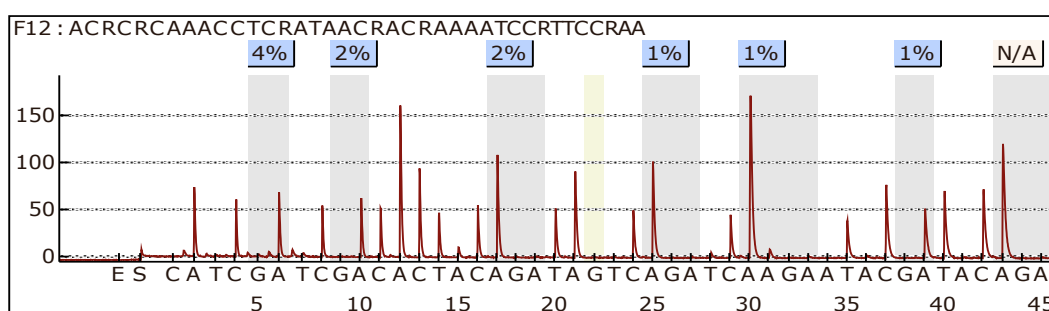


Figure legends

HTR-8/SVneo cells were transfected with siTET3 or siCon. After 48-h post-transfection, Promoter demethylation levels of *DUSP2*, *DUSP4* and *DUSP5* genes detected by pyrosequencing. The methylation levels of the CpG sites in the *DUSP2*, *DUSP4*, and *DUSP5* genes are shown.

Supplemental file 6: Single-nucleotide resolution genome-wide DNA methylation profiling (GEO: GSE117190) after TET3-knockdown in primary human leiomyoma cells.

DUSP2

(+1)

TTAACCCGGGCCCGCCGCGGAGGGCGCCCGGAGTCGACCGCTCGGGCAGCGCCACCGCCACGAGAGCCCC
GGACGCGGGAAAGACCGAAAGGAAGAGGAAGAGGCACCGGTGGCCATGGGGCTGGAGGCGGC (10%-
23%) GCGCGAGCTGGAGTGC (0%-23%) GCGGC (0%-15%)
GCTGGGCACGCTGCTGCGGGATCCGCGGGAGGCGGAACGCA (+193)

DUSP4

(-578) AAACCTACGGGGCTGTCACGCGGGGAAGC (52%-87%)

GCGAAGGTGCCAAGGGATGAAAGCTCAAACCCGAGCCCTGGCCTCCTCAGC (11%-33%)
CGGCTATTTCTTTGGCGCCGCCCGCTAGCGGCGGGGTGCAGCGGCGGCACAGGTGCCGGTGTCCGGG
TGGAGGCGCGGCGCAGGCTGGGCCCGCGGGTAGACGGCGAAAGGC (77%-91%)
GCCGCGGCTCCATTACAAAAGTCCGGGCGCTGCCCGCCGCTGGCGGCGGGTC (0%-11%)
GGAGGCCGCTCCCTCTTCTCTCGGCCTCGGTTTTATGAATGGGCCTGATG (-280)

DUSP5

(-671)

TCACCGCCGACCCCAACCCCGTTTTACTTTTACAACTTTATTATGAAAAATATCAAACATACAGA
AAAGTGGAGAAAACAGTATAACGAATCCGGCCACCCATCACCCAGCCTCAGCGATGACCAACCCGCGCC
TGACCTCTCCAGTCATCTATAACCCACCCCTCGAGGCAAATCTCC (0%-18%) GAC (0%-12%)
GTCCTCTCCTTACACGC (0% -10%) GCAGACCTCGGTAGCGACGGGAATCC (0%-9%)
GTTCCGACTCCTCTGGGGCCCTGGCCGGCTCCCTCGGCCTGCTC (-397)

Figure legends

Sequences of promoter region of DUSP2, DUSP4, and DUSP5. The differentially methylated CpGs are highlighted in red. Purple numbers mark percentage of methylation in siCon (left) or siTET3 (right) transfected leiomyoma cells as determined by genome-wide single-nucleotide-resolution methylation analysis. Blue numbers indicate positions relative to the transcriptional start sites (+1). ChIP-qPCR amplified regions are underlined.

Supplemental file 7: Immunohistochemistry staining (IHC) using antibodies against FOXP1, TET3 and DUSP5 in rat model placenta.

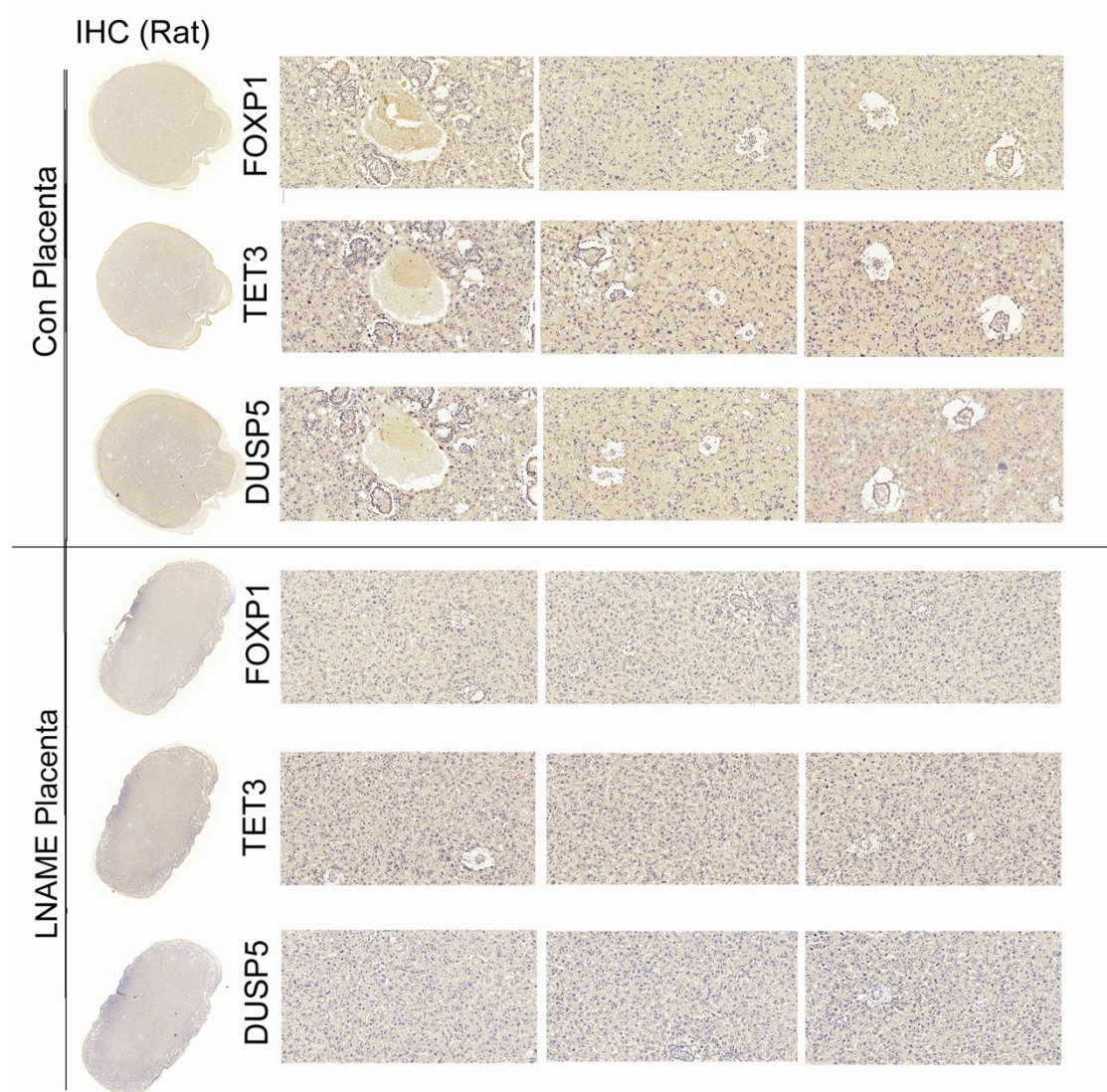


Figure legend:

Six images on the left show representative photomicrographs of hematoxylin-eosin-stained placenta sections of saline- or L-NAME-treated rats on GD 18.5. Eighteen images on the right show immunohistochemistry staining of placental tissues using antibodies against FOXP1, TET3, and DUSP5. Magnification, 20x; Scale bar, 100 μ m. The abundance of FOXP1, TET3, and DUSP5 protein was detected by immunohistochemistry

Supplemental file 8: EDITORIAL CERTIFICATE.



Supplemental file 9: Detailed process of RNA pulldown assays.

RNA pulldown assay

1. Plasmid templates Linearization

Prepare reagent supplies: Sense RNA Plasmid、Antisense RNA Plasmid、Restriction Enzyme Digestion、Ultrapure water、Buffer

1. Thaw the frozen reagents

2. Assemble transcription reaction at room temp

Component	Amount
Ultrapure water	to 50 μ L
Buffer	5 μ L
Plasmid	1 μ g
Restriction Enzyme Digestion	1 μ L

3. Mix thoroughly, Incubate at 37°C, 2 hr

4. Agarose gel electrophoresis confirmed adequate digestion

5. Expand the optimized reaction system

6. Heat inactivation 65°C for 20 min

7. Proteinase K、0.5% SDS for 30 min at 50°C, follow this with phenol/chloroform extraction (using an equal volume).
8. 2 volumes of ethanol precipitation. Mix well and chill at –20°C for at least 15 min.
9. Then pellet the DNA for 15 min in a microcentrifuge at top speed. Remove the supernatant, Resuspend in dH2O or TE buffer at a concentration of 0.5–1 µg/µL.

2. RNA Transcription in Vitro

Prepare reagent supplies: mMESSAGE mMACHINE® Kit AM1344、DNA template、EP tube

1. Thaw the frozen reagents

Place the RNA Polymerase Enzyme Mix on ice, it is stored in glycerol and will not

be frozen at –20°C.

Vortex the 10X Reaction Buffer and the 2X NTP/CAP until they are completely in solution. Once thawed, store the ribonucleotides (2X NTP/CAP) on ice, but keep the 10X Reaction Buffer at room temperature while assembling the reaction.

All reagents should be microfuged briefly before opening to prevent loss and/or contamination of material that may be present around the rim of the tube.

2. Assemble transcription reaction at room temp

The following amounts are for a single 20 µL reaction. Reactions may be scaled up

or down if desired

Component	Amount
Nuclease-free Water	to 20 µL
2X NTP/CAP	10 µL
10X Reaction Buffer	2 µL
(optional) [α -32P]UTP as a tracer	(1 µL)
linear template DNA†	0.1–1 µg
Enzyme Mix	2 µL

3. Mix thoroughly

Gently flick the tube or pipette the mixture up and down gently, and then microfuge tube briefly to collect the reaction mixture at the bottom of the tube.

4. Incubate at 37°C, 2 hr

Typically, 80% yield is achieved after a 1 hr incubation. For maximum yield, we recommend a 2 hr incubation. Since SP6 reactions are somewhat slower than T3 and T7 reactions, they especially may benefit from the second hour of incubation.

5. (optional) Add 1 µL TURBO DNase, mix well and incubate 15 min at 37°C

This DNase treatment removes the template DNA. For many applications it may not be necessary because the template DNA will be present at a very low concentration relative to the RNA.

a. Add 1 µL TURBO DNase, and mix well.

b. Incubate at 37°C for 15 min.

3. Purification for RNA Transcription Reactions

Prepare reagent supplies: MEGAclean™ Kit AM1908

1. Bring the RNA sample to 100 µL with Elution Solution. Mix gently but thoroughly

2. Add 350 µL of Binding Solution Concentrate to the sample. Mix gently by pipetting.

3. Add 250 µL of 100% ethanol to the sample. Mix gently by pipetting.

4. Pipet the RNA mixture onto the Filter Cartridge. Centrifuge for ~15 sec to 1 min, or until the mixture has passed through the filter. Centrifuge at RCF 10,000–15,000 × g (typically 10,000–14,000 rpm).

5. Wash with 2 × 500 µL Wash Solution.

6. Elute RNA from the filter with 50 µL Elution Solution using one of the methods

described below; they are equivalent in terms of RNA recovery.

a. Pre-heat 110 µL of Elution Solution per sample to 95° C.

b. Apply 50 µL of the pre-heated Elution Solution to the center of the Filter Cartridge, close the cap of the tube and centrifuge for 1 min at room temperature (RCF 10,000–15,000 × g) to elute the RNA.

c. To maximize RNA recovery, repeat this elution procedure with a second pre-

heated 50 μ L aliquot of Elution Solution. Collect the eluate into the same Collection/Elution Tube.

7. (optional) Precipitate with 5 M Ammonium Acetate. To concentrate the RNA, precipitate as follows:

a. Add 1:10 volume of 5 M Ammonium Acetate (NH₄Ac) to the purified RNA.

Note: If the sample was eluted with 100 μ L Elution Solution as suggested,

this will be 10 μ L of 5 M NH₄Ac.

b. Add 2.5 volumes of 100% ethanol (275 μ L if the RNA was eluted in 100 μ L).

Mix well and incubate at -20°C for 30 min.

c. Microcentrifuge at top speed for 15 min at 4°C or room temperature (RT).

d. Carefully remove and discard the supernatant.

e. Wash the pellet with 500 μ L 70% cold ethanol, centrifuge again and remove

the 70% ethanol.

f. To remove the last traces of ethanol, quickly re-spin the tube, and aspirate any residual fluid with a very fine tipped pipette, or with a syringe needle.

g. Air dry the pellet. Resuspend the pellet using the desired solution and volume.

4. Pierce RNA 3' End Desthiobiotinylation

Prepare reagent supplies: Pierce RNA 3' End Desthiobiotinylation Kit, 1-50pmol of RNA for labeling, Heated mixer/chiller for incubation at $37^{\circ}\text{C}/16^{\circ}\text{C}$, Chloroform:isoamyl alcohol (24:1), Nuclease-free pipette tips and tubes, 5M NaCl, Ultrapure water, 100% ethanol, ice-cold, 70% ethanol, ice-cold

1. Thaw all kit components except the PEG 30% and DMSO on ice. Thaw DMSO at room temperature and warm the PEG 30% at 37°C for 5-10 minutes until volume is fluid.

2. Adjust the heating block to 85°C .

3. Transfer 5 μ L of the Non-labeled RNA Control to a microcentrifuge tube. Heat the RNA for 3-5 minutes at 85°C . Place RNA immediately on ice.

Note: The RNA may require heating to relax the secondary structure. Also, heating the RNA in the presence of ~25% DMSO may increase efficiency for RNA with significant secondary structure.

4. Prepare the labeling reaction for the control system or test RNA by adding components in the order listed in Table 1.

Note: The last added reagent is PEG 30%. Carefully pipette the PEG 30% into the reaction mixture. Use a new pipette tip to mix the ligation reaction after the PEG 30% addition.

Component	Volume (μL)	Final Concentration
Nuclease-free Water	3	---
10X RNA Ligase Reaction Buffer	3	1X
RNase Inhibitor	1	40U
Non-labeled RNA Control or Test RNA	5	50pmol
Biotinylated Cytidine Bisphosphate	1	1nmol
T4 RNA Ligase	2	40U
PEG 30%	15	15%
Total	30	---

5. Incubate the reactions at 16°C for 2 hours for the control RNA. Ligation may require overnight incubation to increase efficiency.
6. Add 70μL of nuclease-free water to the ligation reaction.
7. Add 100μL of chloroform:isoamyl alcohol to each reaction to extract the RNA ligase. Vortex the mixture briefly, then centrifuge 2-3 minutes at high speed in a microcentrifuge to separate the phases. Carefully remove the top (aqueous) phase and transfer to a nuclease-free tube.
8. Add 10μL of 5M NaCl, 1μL of glycogen and 300μL of ice-cold 100% ethanol. Precipitate for ≥ 1 hour at -20°C.
9. Centrifuge at ≥ 13,000 × g for 15 minutes at 4°C. Carefully remove the supernatant, taking care not to disturb the pellet.
10. Wash the pellet with 300μL of ice-cold 70% ethanol. Carefully remove ethanol and air-dry the pellet (~5 minutes).
11. Resuspend the pellet in 20μL of nuclease-free water or buffer of choice.

5. Pierce Magnetic RNA-Protein Pull-Down

Prepare reagent supplies: Pierce Magnetic RNA-Protein Pull-Down Kit, Target RNA for labeling, Chloroform:isoamyl alcohol (24:1), Ethanol, absolute, Cell Lysis Buffer (for preparation of cell lysate), Magnetic separation stand

A. Pre-Washing Streptavidin Magnetic Beads (Optional)

1. Resuspend the beads in the original vial by gentle swirling or rotation.
2. Remove the amount to be treated and transfer to a nuclease-free tube.
3. Place tube on a magnetic stand to collect the beads against the sides of the tube.
4. Wash the beads twice with a 2X volume of 0.1M NaOH, 50mM NaCl (nuclease-free).
5. Wash the beads once in 100mM NaCl.
6. Continue with equilibration of magnetic beads for RNA capture (Section D).

B. Preparation of Cell Lysate

1. Cell lysates may be prepared using standard lysis buffers
2. Ensure the cell lysate protein concentration is greater than 2mg/mL, such that there is significant dilution into the Binding Reaction Buffer.

C. Binding of Labeled RNA to Streptavidin Magnetic Beads

Note: Use a range of 25-100pmol of RNA per 20-50 μ L of magnetic beads. The instructions below use a scale of 50pmol of RNA to 50 μ L of beads.

1. Add 50 μ L of streptavidin magnetic beads to a 1.5mL microcentrifuge tube.
2. Place the tube into a magnetic stand to collect the beads against the side of the tube. Remove and discard the supernatant.
3. Wash with an equal volume of 20mM Tris (pH 7.5). Resuspend beads by pipetting or vortexing.
4. Repeat Steps 2 and 3.
5. Place the tube into a magnetic stand to collect the beads against the side of the tube. Remove and discard the supernatant.
6. Add an equal volume of 1X RNA Capture Buffer. Resuspend beads by pipetting or vortexing.
7. Add 50pmol of labeled RNA to the beads. Mix gently by pipetting.
8. Incubate for 15-30 minutes at room temperature with agitation.

D. Binding of RNA-Binding Proteins to RNA

1. Place the tube into a magnetic stand to collect the beads against the side of the tube. Remove and discard the supernatant.
2. Wash with an equal volume of 20mM Tris (pH 7.5). Resuspend beads by pipetting or vortexing.
3. Repeat Steps 1 and 2.
4. Place the tube into a magnetic stand to collect the beads against the side of the tube. Remove and discard the supernatant.
5. Dilute 10X Protein-RNA Binding Buffer to 1X (i.e., 10 μ L into 90 μ L of ultrapure water for each reaction).
6. Add 100 μ L of 1X Protein-RNA Binding Buffer to the beads and mix well.
7. Prepare a Master Mix of RNA-Protein Binding Reaction (Table 2).

Reagent	Volume (μ L) per 100 μ L reaction for control	Range
10X Protein-RNA Binding Buffer	10	5-20 μ L
50% glycerol	30	0-50 μ L
Lysate (protein conc. > 2mg/mL)	1-30	20-200 μ g
Nuclease-free water	to 100	to 100 μ L

8. Place the tube into a magnetic stand to collect the beads against the side of the tube. Remove and discard the supernatant.
9. Add 100 μ L of Master Mix to the RNA-bound beads. Mix by pipetting or gentle vortexing.
10. Incubate 30-60 minutes at 4°C with agitation or rotation.

E. Washing and Elution of RNA-Binding Protein Complexes

1. Place the tube into a magnetic stand to collect the beads against the side of the tube. Transfer the supernatant to a tube for later analysis.
2. Wash with equal volume of 1X wash buffer (100 μ L).
3. Repeat Steps 1 and 2 two additional times. Save wash supernatants for analysis, if desired.
4. Place the tube into a magnetic stand to collect the beads against the side of the tube. Transfer the supernatant to a tube for later analysis.
5. Add 50 μ L of Elution Buffer to the beads and mix well by vortexing. Incubate 15-30 minutes at 37°C with agitation.
6. Place the tube into a magnetic stand to collect the beads against the side of the tube.
7. Remove supernatant for downstream analysis.

8. If the downstream application is Western blotting, add reducing sample buffer to samples to 1X.

F. Western Blot Analysis

Supplemental table 1: The detailed clinicopathological features of normal pregnancy and preeclampsia

Clinical characteristics of preeclamptic and normal pregnancies.

Variable	PE (N=64)	Normal (N=64)	<i>P</i> value ^a Normal vs P
Maternal age (year)	32±4.95375	34.2968±3.5307	p>0.05
Maternal weight (kg)	76.226±11.1376	74.0703±8.0602	p>0.05
Smoking	1	0	p>0.05
Systolic blood pressure (mm Hg)	162.6718±14.9443	116.1406±7.9758	p<0.01
Diastolic blood pressure (mm Hg)	105.9687±10.8173	71.5843±8.6279	p<0.01
Proteinuria (g/day)	>0.3g	<0.3g	p<0.05
Body weight of infant (g)	2291.9375±9089.06	3385.15±364.243	p<0.05
Gestational age (week)	34.06±3.231	38.375±0.9677	p<0.05

Supplemental table 2: Related antibody information and description.

Gene	Antibody	Concentration	Volume	Source	Species	Abundance	Antigen	Concentration	Volume	Wash
GAPDH	5% nonfat milk	5% nonfat milk	1:2000	CMC TAG, AT0002	5% milk	1:3000	Anti-Rabbit IgG, 1:3000	0.22um 250mA, 100min		
FOXP1	5% nonfat milk	5% nonfat milk	1:750	PROTEINTECH GROUP, 22051-1-AP	5% milk	Anti-Rabbit IgG, 1:3000	Anti-Rabbit IgG, 1:3000	0.22um 250mA, 100min		Wash 3 times after 1st and 2nd Abs, 10 min each time
TET3	5% nonfat milk	5% nonfat milk	1:500	GENE Tex 121453	5% milk	Anti-Rabbit IgG, 1:3000	Anti-Rabbit IgG, 1:3000	0.22um 250mA, 120min		Wash 3 times after 1st and 2nd Abs, 5 min each time
DUSP2	5% nonfat milk	5% nonfat milk	1:750	PROTEINTECH GROUP, 27327-1-AP	5% milk	Anti-Rabbit IgG, 1:3000	Anti-Rabbit IgG, 1:3000	0.22um 250mA, 90min		Wash 3 times after 1st and 2nd Abs, 5 min each time
DUSP4	5% nonfat milk	5% nonfat milk	1:750	PROTEINTECH GROUP, 66349-1-Ig	5% milk	Anti-Mouse IgG 1:3000	Anti-Mouse IgG 1:3000	0.22um 250mA, 90min		Wash 3 times after 1st and 2nd Abs, 5 min each time
DUSP5	5% nonfat milk	5% nonfat milk	1:500	abcam ab 200708	5% milk	Anti-Rabbit IgG, 1:3000	Anti-Rabbit IgG, 1:3000	0.22um 250mA, 90min		Wash 3 times after 1st and 2nd Abs, 5 min each time
foxp2	5% nonfat milk	5% nonfat milk	1:750	PROTEINTECH GROUP, 20529-1-AP	5% milk	Anti-Rabbit IgG, 1:3000	Anti-Rabbit IgG, 1:3000	0.22um 250mA, 100min		Wash 3 times after 1st and 2nd Abs, 5 min each time
TET1	5% nonfat milk	5% nonfat milk	1:500	abcam ab 191698	5% milk	Anti-Rabbit IgG, 1:3000	Anti-Rabbit IgG, 1:3000	0.22um 250mA, 120min		Wash 3 times after 1st and 2nd Abs, 5 min each time
SUV39H1	5% nonfat milk	5% nonfat milk	1:500	abcam ab 12045	5% milk	Anti-Mouse IgG 1:3000	Anti-Mouse IgG 1:3000	0.22um 250mA, 100min		Wash 3 times after 1st and 2nd Abs, 5 min each time

Supplemental table 3: Bioinformatics analysis (<http://bibiserv.techfak.uni-bielefeld.de/mahybrid/>) predicted the binding sites of miR-218 in the 3'-UTR of FOXP1


miRNA	MIMATid	Gene	-Y	EntrezID	RefseqID	mirWalk	Microt4	miRanda	mirbridge	miRDB	miRMap	miRMAP
hsa-miR-218-5p	MIMAT0000	FOXP1		27086	NM_001244808	1	1	0	0	0	1	0
hsa-miR-218-5p	MIMAT0000	FOXP1		27086	NM_032682	1	0	0	0	0	1	0
hsa-miR-218-5p	MIMAT0000	FOXP1		27086	XM_005264740	1	0	0	0	0	1	0
hsa-miR-218-5p	MIMAT0000	FOXP1		27086	XM_005264742	1	0	0	0	0	1	0
hsa-miR-218-5p	MIMAT0000	FOXP1		27086	NM_001244813	1	0	0	0	0	1	0
hsa-miR-218-5p	MIMAT0000	FOXP1		27086	XM_005264731	1	0	0	0	0	1	0
hsa-miR-218-5p	MIMAT0000	FOXP1		27086	NM_001244812	1	0	0	0	0	1	0
hsa-miR-218-5p	MIMAT0000	FOXP1		27086	XM_005264739	1	0	0	0	0	1	0
hsa-miR-218-5p	MIMAT0000	FOXP1		27086	XM_005264741	1	0	0	0	0	1	0
hsa-miR-218-5p	MIMAT0000	FOXP1		27086	XM_005264735	1	0	0	0	0	1	0
hsa-miR-218-5p	MIMAT0000	FOXP1		27086	XM_005264736	1	0	0	0	0	1	0
hsa-miR-218-5p	MIMAT0000	FOXP1		27086	XM_005264733	1	0	0	0	0	1	0
hsa-miR-218-5p	MIMAT0000	FOXP1		27086	NM_001244815	1	0	0	0	0	1	0
hsa-miR-218-5p	MIMAT0000	FOXP1		27086	NM_001244814	1	0	0	0	0	1	0
hsa-miR-218-5p	MIMAT0000	FOXP1		27086	NM_001244816	1	0	0	0	0	1	0
hsa-miR-218-5p	MIMAT0000	FOXP1		27086	XM_005264737	1	0	0	0	0	1	0
hsa-miR-218-5p	MIMAT0000	FOXP1		27086	XM_005264738	1	0	0	0	0	1	0
hsa-miR-218-5p	MIMAT0000	FOXP1		27086	XM_005264732	1	0	0	0	0	1	0
hsa-miR-218-5p	MIMAT0000	FOXP1		27086	XM_005264729	1	0	0	0	0	1	0
hsa-miR-218-5p	MIMAT0000	FOXP1		27086	XM_005264734	1	0	0	0	0	1	0
hsa-miR-218-5p	MIMAT0000	FOXP1		27086	NM_001244810	1	0	0	0	0	1	0
hsa-miR-218-5p	MIMAT0000	FOXP1		27086	XM_005264730	1	0	0	0	0	1	0
hsa-miR-218-5p	MIMAT0000	FOXP1		27086	NM_001012505	0	0	0	0	0	1	0

Supplemental table 4: Target_Primer in methyltarget sequencing.

Target	Chr	Gene	mRNA	mRNA Strand	TSS	TES	Start	End	Length	Target Strand	Distance2TSS	PrimerF
DUSP2_04	chr2	DUSP2	NM_004418	-	9614 5440	9614 3168	9614 5482	9614 5675	194	+	-42	GGTTTTYGGGGTAT ATATAAGGGTAGA
DUSP4_18	chr8	DUSP4	NM_0057158	-	2934 8805	2933 3061	2934 8363	2934 8097	267	-	442	TTGAGYGGGGTTAG TTTTGGTTA
DUSP5_21	chr10	DUSP5	NM_004419	+	1.1E+08	1.11E+08	1.1E+08	1.1E+08	259	+	-100	GTTYGAGGGGYGGC AAATA

Supplemental table 5: Pyrosequencing related primer data.

1. DUSP2

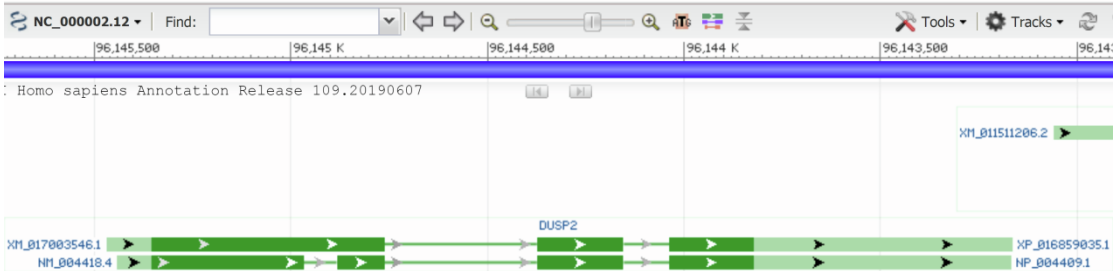


Genomic regions, transcripts, and products

Go to [reference sequence](#)

Genomic Sequence: NC_000002.12 Chromosome 2 Reference GRCh38.p13 Primary Assembly

Go to nucleotide: [Graphics](#) [FASTA](#) [Gen](#)



mRNA `join(1..708,1096..1315,1432..2303)`
`/transcript_id="XM_017003546.1"`
`/db_xref="GeneID:1844"`

CDS `join(115..708,1096..1315,1432..1646)`
`/gene="DUSP2"`
`/gene synonym="PAC-1; PAC1"`
`/protein id="XP_016859035.1"`
`/db_xref="GeneID:1844"`
`/db_xref="HGNC:HGNC:3068"`
`/db_xref="MIM:603068"`

ORIGIN

```
1 ttaaccCGgg cCGcCGCGga gggCGccCGg agtCGacCGc tCGggcagCG
ccacCGccac
61 gagagccCGg gaCGCGggaa agacCGaaag gaagaggaag aggcacCGgt
ggccatgggg
```

NOTES: -2000bp+5 'UTR+some CDSsequences (ATG are marked in green), and methylation islands are marked with horizontal lines

Homo sapiens chromosome 2, GRCh38.p13

Primary Assembly

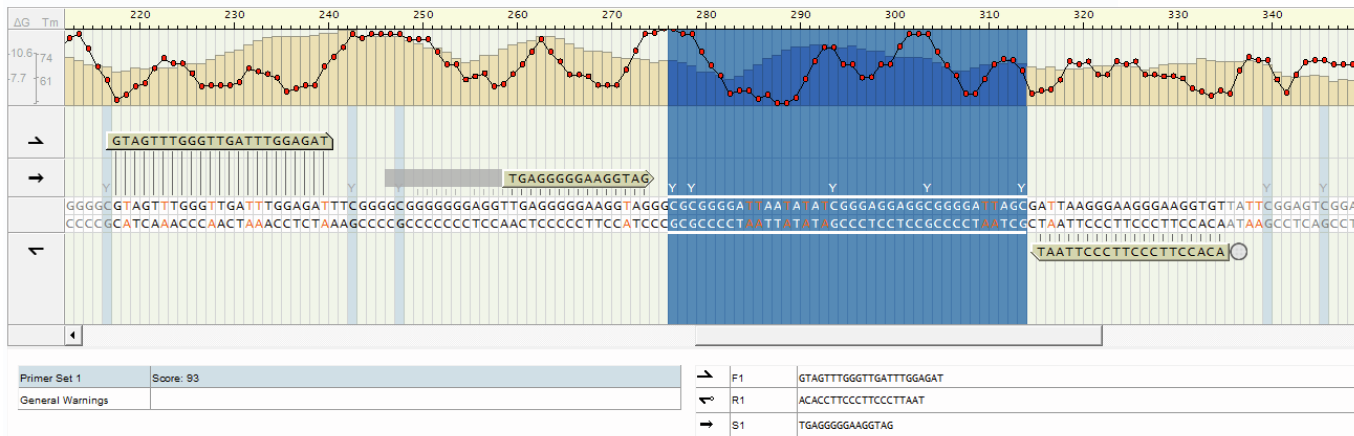
NCBI Reference Sequence: NC_000002.12

[GenBank Graphics](#)

>NC_000002.12:c96147468-96143166 Homo sapiens chromosome 2, GRCh38.p13 Primary Assembly

CCCCACATGCAGAACTCCC**CG**GCAAGGTATACCAGATTCTCCAGAAGGAGGGGAAGAGGCCAGCCAG
CATGGGAGTTGGGTCTGGAGCCCCTTACA**CG**GCTGAGCTGAATTCACCTCCTGAATCAGGGATCCCACCT
GGCTGGGGTCTCCACAGAGCTGGAAGGCTTTGGCTCCTGGCCCAGCAGCAAGACTGGACCTGATTGT
CCTTCTGCA**CG**CTCTGTAATTTGCCCTGGAATAAGCATTAAGTCATTTGGAGGC**CG**ATGCCAAAGATA
AGGGCTCATATCAGCCTTTGGGATCTGTGGCCAGACTCCCTGGCTCTGTTGTGGGCTTTGCTGCCTCA
GCCTCCAGACTGGCCTGCCAGGGACAG**CG**GGGCTCAGCCAAGTTGCCCAGACAGTGGAGTAGCCTTAG
AG**CG**TTGGAGCCAGTGTGGAAGAGC**CG**CTGCACCATGATGTGCTCCCTTACAGATGGAGACACTGAGA
GGGTGACGTGGCCCCAGGGACCTTTGGAGTCCTTGGGGCTTTTCTCCTCTGCAT**CG**GCTCTGACCCAG
CACACACAAGCTCCAGCTCCTTCTCACACATAGTGAACTGCACAGGTA**CG**ATGCTGCCCTGCACACAA
CCAGGCATACAGCACACTGCTGTGAGGAACTCAGGGCAGACAAGTCCAGAAGGGCT**CG**GGCTCTCCAC
AGGTCCCAGCTGTCACTCTTCAAGA**CG**GTCTGGACACAGGGGTCTGTGGGGGAGC**CG**GAAGGGTCTTTC
AGAGGGCA**CG**GAGGAGGGCCTCAGGAGACTGGGGCTTGAGGGTGGTTCTGAAATCCCA**CG**CAGCTG
GGGGCAGGG**CG**AGGGCAGCTCCAG**CG**CAGTGA**CG**CTGTCTCCACCCACCTCAACTTCTCTGCTTGAGTT
TGGGAGTTCACTGCCAACAAATTTCTGTGGCTCAGACACCCCA**CG**CACACCTGGGCCCTACCACATC**CG**G
CAGCAGGGCTGGGGGAGGG**CG**GAATGGAGGGGATACCCAGGCCCCAGTCTC**CG**GGTGCAGTGCCTAGC
CCTGGACTTTGCTGCC**CG****CG**GGGCTGGACAGGGAGGCCTAGGATGGGGGAGGCCAGTTCTGTTCTGCT
TCTCCCTCTTCCCTTGCCAAGGTCTTGAATCC**CG**CAGGCTGGGGAGGG**CG**GGAG**CG**TCAG**CG**GA
CTTCCCTCCAGGG**CG**GGCTTGTGGCAGGGGGAAGTACTTCTCTCTGGGGCTGGGGGCTTTCCCTGCAC
CCAGGAGGAAGAAGCTTTGCCCTACACATAACTGGAAACCAGTCACAGACCCCTGCTTTCCCATGAAA
GGCCCTGGGACCCCCCTCATTTCCCTT**CG**GCCAAGCCCAGGGCCTGGGCC**CG**GGGACTGTGTTCT
GGCCTAGCTTGGCCACCAACCTACTGCAAGACCCTGAGTACTGGTCTTATCCAGGCAATGGGGGGTGGG
GAGGGGAGGAGAGAGAAAGTCCCTCTGGCTCAAGGTCTCCAAATAGATGAGAAATAGGACATCTCAGC
AGGGACCCCCCATCATCCAGTGTAGAAATCACC**CG**TGGCAGCAGGCATTTGTCAATGTTTGTGGTGA
CAAATTTCTAAGAGGAAAATTTCTGGGAGGGAAAAGGAAAAGGCAGAGGAAG**CG**TGGGGTTAGGGGTGG
GGTACTCCAAGGGTCAT**CG**TTGGCCCTAAAGGGGGACCTGCATCTGAGAAGCTGGGTTCGCCAGGACTG
AGTGGCTTGGGACAGGTCAAAGGGTGGG**CG**CAAAA**CG**GAGGGGTGCTAGTCCCTC**CG**ACTC**CG**GGTAA
CACCTTCCCTTCCCTTAGT**CG**CTGGTCCC**CG**CCTCCTCC**CG**GTGTGTTGGTCCC**CG**CG**CG**CCCTGCCTTC
CCCCTCAACCTCCCCC**CG**CCC**CG**AAGTCTCCAGGTCCAGCCAGACTG**CG**CCCCA**CG**TGAGGGG**CG**GG
CG**CG**GG**CG**CG**CG**GG**CG**CCAG**CG**CCCTCCTGCTCTGCCCTTGTATGGTGGCC**CG**GAGGC**CG**GCCCA**CG**GGT
ACTTAACC**CG**GGC**CG**CC**CG**CGAGGG**CG**CC**CG**GAGT**CG**AC**CG**CT**CG**GGCAG**CG**CCAC**CG**CCA**CG**AGAGCC
CGGGAA**CG**CGGGAAAGAC**CG**AAAGGAAGAGGAAGAGGCAC**CG**GTGGCC**AT**CGGGCTGGAGG**CG**G**CG**CGC
AGCTGGAGTG**CG**CG**CG**CTGGGCA**CG**CTGCTG**CG**GGATC**CG**CGGGAGG**CG**GAA**CG**CA**CG**CTGCTGCTGG
ACTGC**CG**CCCCCTTCTGGCCTTCTGC**CG****CG**CCACGTG**CG**CG**CG**CGCGGCCAGTGCCTTGGA**CG**CGC
TGCTG**CG**CG**CG**CGCGCGCGGCCCTCCTGC**CG**CGTTCT**CG**CCTGCCTGCTGCC**CG**AC**CG**CGCGCTGC
GGA**CG**CGCCTGGTC**CG**CGGGGAGCTGG**CG**CGGGC**CG**TGGTGTGGAA**CG**AGGGCAGTGCCT**CG**GTGG**CG**G
AGCTC**CG**GCC**CG**ACAGCC**CG**GCTCATGTGCTGCTGGCCG**CG**CTGCTGCA**CG**AGACC**CG**CGCGGGGCCCA
CTGC**CG**TGTACTTCTG**CG**AGGTGAGCAAGC**CG**GC**CG**CCCTTGGCC**CG**CCCCACC**CG**ACTCCAGCC**CG**G
CTTTCCCTGCTGAT**CG**TGCTCTTCCCTCCTTGCAGGAGGCTT**CG**A**CG**GTTCAGGGCTGCTGTCC**CG**
ATCTGTGCTCTGAGGCCCC**CG**CCCCTG**CG**CTGC**CG**CAACAGGGGACAAAACCAGC**CG**CTC**CG**ACTCCA
GGGCTCCTGTCTA**CG**ACCAGGTGAGTATTGACCCCCCTCCC**CG**AACCTCCCTCTCTCCC**CG**CGCGGA
CTGGG**CG**CCTCTAGGGAAAGAGCCTGCCATTTGGGGATG**CG**AGCAGTTTGGCCATATACACACACTTTT
ATA**CG**TGTGTGTTGGGGAGGGGTGGGGCATGGCTGCT**CG**CG**CG**TGCCCTGTATGGGTCTGTGTATG
TTTGCATGTGTATGTTGGGAGCATGAAGGGAAAATGTATGTCC**CG**GTGTGTCCTC**CG**CACATTCCTGAGA

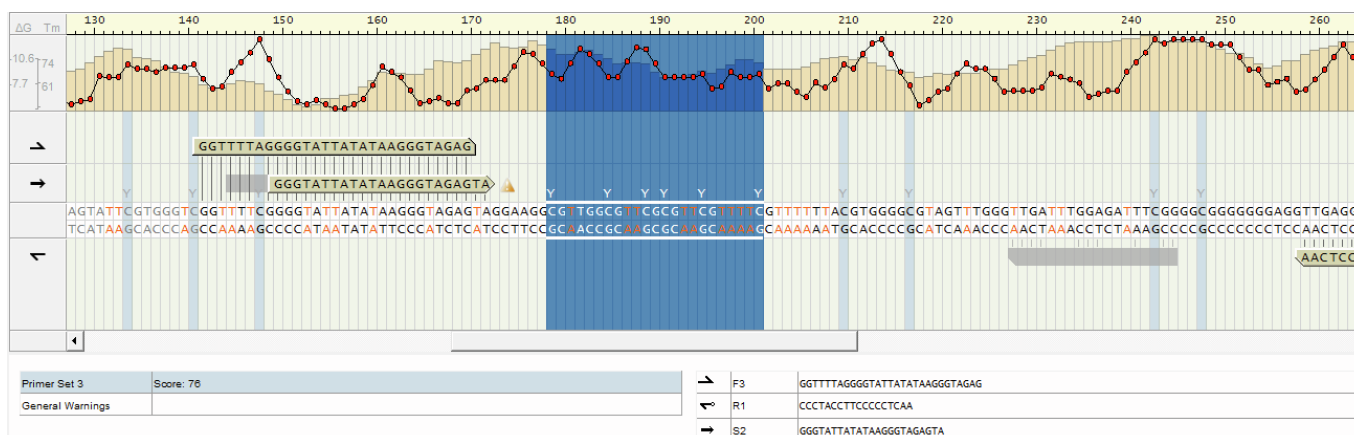
CCTGTCTCAGGTCAGGAGGACTGGCTGAGGAGTCTCTTGTCTCGGCCAGCCCATGGGGTCTCCACCCG
 CTGCTGCTCCAGCTCTCAGGGGCTGGGCTGGAAAGCCTCACGCC



Primer Set 1	Score: 93
General Warnings	

F1	GTAGTTGGGTTGATTGGAGAT
R1	ACACCTTCCCTCCCTTAAT
S1	TGAGGGGAAGGTAG


	PCR Product	Forward PCR Primer, F1	Reverse PCR Primer, R1	Sequencing Primer, S1
Length, nt	118	23	20	15
Position, 5'- 3'		217 - 239	334 - 315	259 - 273
Warnings				
Tm, °C		59.7	61.1	49.1
%GC	50.8	39.1	45.0	60.0
Sequence to Analyze	GGYGYGGGA TTAATATATY GGGAGGAGGY GGGATTAGY GATTAAGGGA AGGGAAGGTG TTATT			



Primer Set 3	Score: 76
General Warnings	

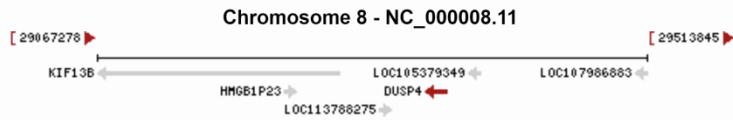
F3	GGTTTTAGGGGTATTATATAAGGGTAGAG
R1	CCCTACCTTCCCCCTCAA
S2	GGGTATTATATAAGGGTAGAGTA

	PCR Product	Forward PCR Primer, F3	Reverse PCR Primer, R1	Sequencing Primer, S2
--	-------------	------------------------	------------------------	-----------------------

Length, nt	135	29	18	23
Position, 5'- 3'		141 - 169	275 - 258	149 - 171
Warnings				 A homopolymer is detected adjacent to polymorphi
Tm, °C		58.8	58.7	45.9
%GC	45.2	37.9	61.1	34.8
Sequence to Analyze	GGAAGGYGTT GGYGTTYGYG TTYGTTTTYG TTTTTAYGT GGGG			

2. DUSP4

109.20190607	current	GRCh38.p13 (GCF_000001405.39)	8	NC_000008.11 (29333062..29350684, complement)
105	previous assembly	GRCh37.p13 (GCF_000001405.25)	8	NC_000008.10 (29190579..29208267, complement)

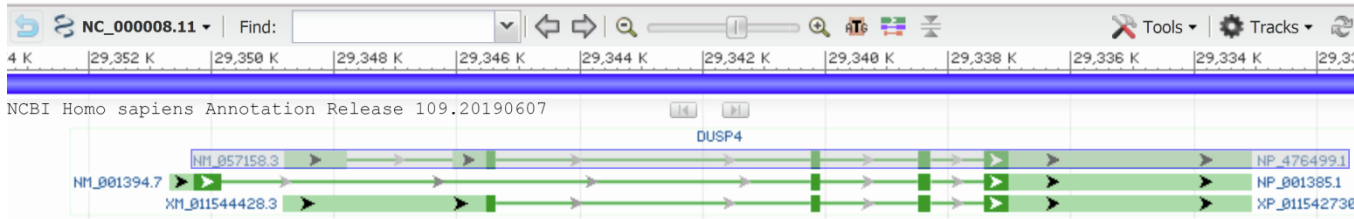


Genomic regions, transcripts, and products

Go to [reference sequence](#)

Genomic Sequence: [NC_000008.11](#) Chromosome 8 Reference GRCh38.p13 Primary Assembly

Go to nucleotide: [Graphics](#) [FASTA](#) [G](#)



mRNA [join\(1..839,10442..10587,12184..12403,13274..17621\)](#)
 /gene="DUSP4"
 /gene synonym="HVH2; MKP-2; MKP2; TYP"
 /product="dual specificity phosphatase 4,
 transcript
 variant 1"
 /note="Derived by automated computational
 analysis using
 gene prediction method: BestRefSeq."
 /transcript id="NM_001394.7"
 CDS
[join\(407..839,10442..10587,12184..12403,13274..13659\)](#)
 /gene="DUSP4"
 /gene synonym="HVH2; MKP-2; MKP2; TYP"
 /note="isoform 1 is encoded by transcript
 variant 1;

Derived by automated computational analysis
using gene
prediction method: BestRefSeq."
/codon start=1
/product="dual specificity protein phosphatase 4
isoform
1"
/protein id="NP_001385.1"

1 ctggctgggg cagtgcCGctg agCGcCGgag gagCGtaggc agggcagCGc tggCGccagt
361 tctcttctct tctcCGCGCG cccagcCGcc tCGgttccCG gCGaccatg tgaCGatgga

Homo sapiens chromosome 8, GRCh38.p13

Primary Assembly

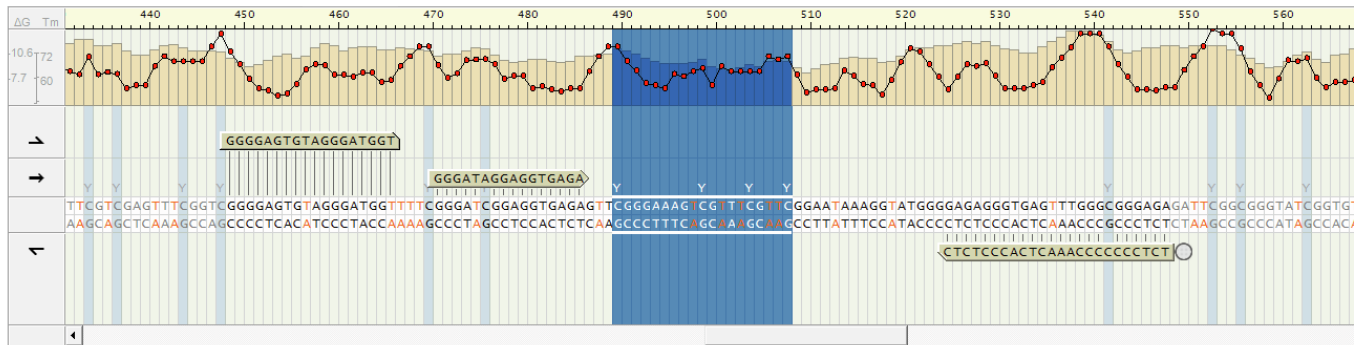
NCBI Reference Sequence: NC_000008.11

[GenBank Graphics](#)

>NC_000008.11:c29352684-29333062 Homo sapiens chromosome 8,
GRCh38.p13 Primary Assembly

GGCCACGCCGTGCGGCTTTGACCACTGATCTCCACCCCGGAGTGCCCGACGCCAGGGTCTTGCC
ACCGGGCAGCCTCGGTCAGTCCACAGTTGTGGCTCCTTCCAGGGCCTGGACTAGGGTGAGCACAAGCCT
TGAGCGCAACATTTAAGAAGGGCGCGAAAAAGTCAGTAATCAAAGAAATATCTTGATGCAATGCCTCT
TTAAAAGAAAAAATGCAAAAAATCCATGATGAATAAAATACTAAATTTTAAAAGAGAAAGGATCC
GTGCAGTGCCATCGTAAGCCATTTTGGAGCCCGGAGCAAAAGGAAATATCACCTTGCCCAAGCGGTGCC
CCTACAGCTCATCCGAGTAGGGCCCGGGGTCGAGGCATTCGGGCCCAGTGGGGGACGAGGCCAGTCG
AAGGTCTCGGAAGTGAGGCTCCGCGAGCTCCGGTCGGGGAGTGCAGGGATGGCCCCCGGGACCGGAG
GTGAGAGCTCGGGAAAGCCGCTCCGCCGAACAAAGGCATGGGGAGAGGGTGTGCTTGGGCGGGAGA
GACCCGCGGGTACCGGTGCCCTCGCTGCCTGGGTCGGGCTTCCACGCGCGCCCCGGAATGGAATACCGC
TACTCTGCAGCCTCCGAAACTGCGAGCGAGTCTGTAACTCCCTTGCTCTGTGATTAATTCTCACTAAC
AAGACTTGGCAAGATGTCGGGCGAATGATTTTGGCTTCTGCACGTCCCACCGCGTCGTGCACAAA
CCCCCAGCCAAAAGCCGCTCTGGGAAATTTAAATGCAAAAGAGAAATGGGGATGGGGAGGGCTGCTACCG
TGACCAGGAAAAAGGGATGCCAGAAACATGAATCGGACCCAGAGCTGCTGAAGTCCTTTCAAAGGTC
ATTCTTTGCGGGTACATTTTCCAGGGTCCAGCTCCGCAACAAATGTGGACCCTGTCAATTTCTGAAAGG
ATAATTACAACATATGCAAGATAGGGTGAAGACGTTTCCCAAACCCGAAAACCTTGTTTTTCCCCCGAC
CAGGGTTAAATAAACATCTTTTAGGAAGCGTGGACAGGAGCGCAGCCTGCTCTCCTCCCTCGGAACACC
ATTCCGGCAATTAATGCCTCCCTTTGGGTAGTAAAGCAACAAACCCACACCTCACTCCGATCCTGGGC
TTCGGGCGGGAGGACTTCTCTTTCATCTTCCAAGCAGGGGTTGCCACGTTCTTGGGGAAGCTATAA
AACTGATTTAATGGCTTTAGATGAAAATCGATCACGCTAATGCATACGCTAACGTCTCAGGAATCGCAT
ATTCAGAAAGGACTGGCCGGGCCGAAAGCGCACGGGGAGTCTGGGGCTAGGAGGTGTCAGGCCCGCTG
GGTGGCAGCAGCGCTCCGGTCCCCTCTCCACTTGGGTAACCGGGAAAAACCTACCGGGGCTGTCACGCG
GGGAAGCGCGAAGGTGCCAAGGGATGAAAAGCTCAAACCCGAGCCCTGGCCTCCTCAGCCGGCTATTTCC
TTTGGCGCCCGCCTAGCGCGGGGTGCAGCGCGGCACAGGTGCCGGTGTCGGGCTGGAGGCGCG
CGCAGGCTGGGCCCGCGGGTAGACGCGAAAGCGCCGCGCGCTCCATTCAAAAGTCGGGCGCTGCC
CGCGCTGGCGGGGGTCGGAGGCCGCTCCCTCTTCTCTCGGCCTCGTTTTATGAATGGGCCTGAT
GCGAGCACCCGCGCCCTGTTTACTCCGCTTTTGTGAGCGTCGAGTCCCGTGACCGGGAGCCAGCGG

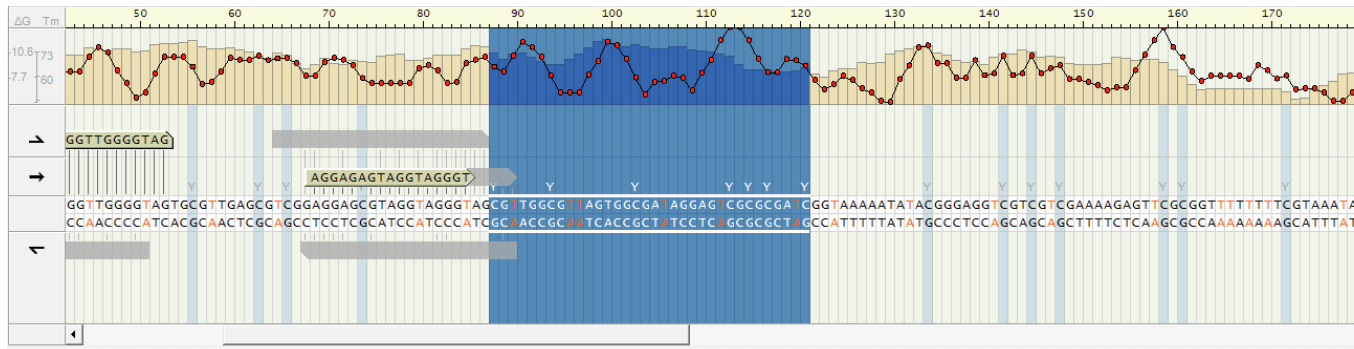
CGCGCTCCATTCAAGCTC**CG**GGGAGGGGGTGGGAGGAGGGGCC**CG**GAGGGGG**CG**GGGAGTCAG**CGCG**
 GGGG**CG**GGGGACAG**CGCG**GGGG**CG**GGGA**CG****CGCG**GGGCC**CG**GAATGGAA**CG**GGG**CG**GGCC**CG**
 GGGTAGTACCTAG**CG**CCCCCTCCCC**CG**GGAG**CGCG**GAGGAGCATTAATAAACCTCTAAGC**CG**AGGAGAA
 AACTCTGGCTGGGGCAGTG**CG**CTGAG**CG****CG**GAGGAG**CG**TAGGCAGGGCAG**CG**CTGG**CG**CCAGTGG**CG**
 ACAGGAGC**CGCGCG**AC**CG**GCAAAAATAC**CG**GGAGGCC**CG**T**CG**CCGAAAAGAGT**CG**CGGTCTCTCTC
GTAAACACACTCTCTCCAC**CG****CG**CCTCCCCCTC**CG**CTCTG**CG****CG****CG**CC**CG**GTGGG**CG**CC**CG**AGGC
CGCTC**CG**ACTGCTATGTGAC**CG**CGAGGCTG**CG**GGAGGAAGGGACAGGGAAGAAGAGGCTCTCC**CGCG**
 GAGCCCTTGAGGACCAAGTTTG**CG**GCCACTTCTGCAGG**CG**TCCCTTCTTAGCTCT**CG**CC**CG**CCCCTTTC
 TGCAGCCTAGG**CG**GCC**CG**GGTTCTTCTCTTCTCCT**CGCGCG**CCAGC**CG**CCT**CG**GTTC**CG**CGACC**A**
TGGTGAC**CG**ATGGAGGAGCTG**CG**GGAGATGGACTGCAGTGTGCTCAAAGGCTGATGAAC**CG**GGAC**CG**AG
 AATGG**CG**GG**CG****CGCG**GG**CG**GCAG**CG**GCAGCCA**CG**GCACCCTGGGGCTGC**CG**AG**CG**GG**CG**GCAAGTGCCTG
 CTGCTGGACTGCAGAC**CG**TTCC**CG**CGCACAG**CGCG**GGCTACATCCTAGGTT**CG**GTCAA**CG**T**CG**CTGT
 AACACCAT**CG**TG**CG**GG**CG**GGCTAAGGGCTC**CG**TGAGCCTGGAGCAGATCCTGCC**CG**CGAGGAGGAG
 GTA**CGCG**CC**CG**CTTG**CG**CTC**CG**CCCTACT**CG**GG**CG**GT**CG**CTACGAC**CG**AG**CG**CAGCC**CGCGCG**CC
GAGAGCCTC**CGCG**AGGACAGCAC**CG**TGT**CG**CTGGTGGTGCAGG**CG**CTGCGC**CG**CAAC**CG**CGAG**CG**CACC
GACATCTGCCTGCTCAAAGGTA**CG**AGGGCTC**CG**GG**CG**CTAGCTGGAGT



Primer Set 1	Score: 89
General Warnings	

→ F1	GGGAGTGTAGGGATGGT
← R1	TCTCCCCCAAACTCACCTCTC
→ S1	GGGATAGGAGGTGAGA

	PCR Product	Forward PCR Primer, F1	Reverse PCR Primer, R1	Sequencing Primer, S1
Length, nt	100	18	24	16
Position, 5'- 3'		448 - 465	547 - 524	470 - 485
Warnings				
Tm, °C		62.1	63.1	42.8
%GC	49.0	61.1	62.5	56.3
Sequence to Analyze	GTTYGGGAAA GTYGTTTYGT TYGGAATAAA GGTATGGGA GAGGGTG			



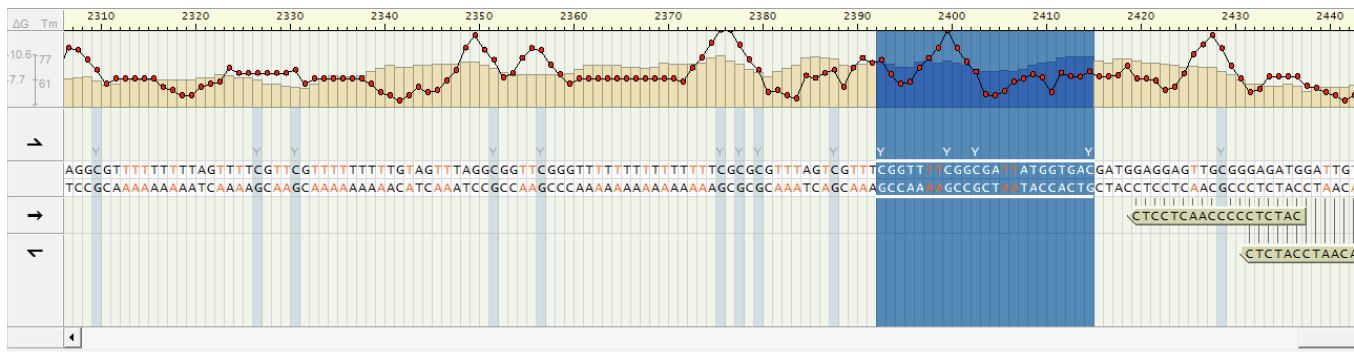
Primer Set 2	Score: 80
General Warnings	

F1	GGAGAAAAATTTGGTTGGGGTAG
R2	TCTTCTCCCTATCCCTTCTCTC
S2	AGGAGAGTAGGTAGGGT

Primer Set 2	Score: 80
General Warnings	

F1	GGAGAAAAATTTGGTTGGGGTAG
R2	TCTTCTCCCTATCCCTTCTCTC
S2	AGGAGAGTAGGTAGGGT

	PCR Product	Forward PCR Primer, F1	Reverse PCR Primer, R2	Sequencing Primer, S2
Length, nt	267	23	23	17
Position, 5'- 3'		30 - 52	296 - 274	68 - 84
Warnings	Deviation from optimal amplicon size			
Tm, °C		60.8	62.7	46.1
%GC	36.7	43.5	52.2	52.9
Sequence to Analyze	AGYGTGGYG TTAGTGGYGA TAGGAGTYGY GYGATYGGTA AAAATATA			



Primer Set 1	Score: 73
General Warnings	

F1	AAGGGGATAGGGAAGAAGAG
R1	CCTTTTAAACACTACAATCCATCTC
S1	CATCTCCCCCAACTCTC

Primer Set 1	Score: 73
General Warnings	

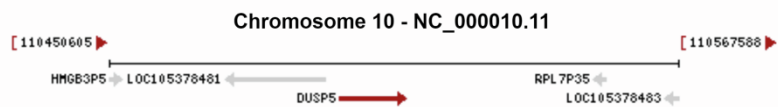
F1	AAGGGGATAGGGAAGAAGAG
R1	CCTTTTAAACACTACAATCCATCTC
S1	CATCTCCCCCAACTCTC

	PCR Product	Forward PCR Primer, F1	Reverse PCR Primer, R1	Sequencing Primer, S1
Length, nt	219	20	27	18
Position, 5'- 3'		2239 - 2258	2457 - 2431	2436 - 2419

Warnings				
Tm, °C		59.9	60.3	45.7
%GC	32.4	50.0	37.0	61.1
Sequence to Analyze	CATCRTACC ATAATCRCCR AAAACCRAAA CRACTAAAC			

3. DUSP5

105 previous assembly GRCh37.p13 (GCF_000001405.25) 10 NC_000010.10 (112257625..112271302)

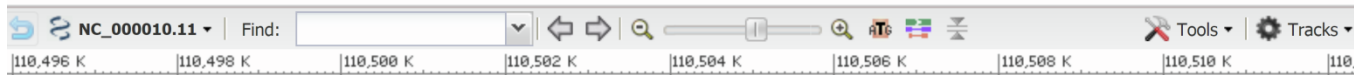


Genomic regions, transcripts, and products

Go to [reference sequence](#)

Genomic Sequence: NC_000010.11 Chromosome 10 Reference GRCh38.p13 Primary Assembly

Go to nucleotide: [Graphics](#) [FASTA](#)



NCBI Homo sapiens Annotation Release 109.20190607

16.2 NM_004419.4 DUSP5 NP_004419.4

mRNA join(1..594,4815..4963,9029..9248,12114..13627)

/gene="DUSP5"

/gene synonym="DUSP; HVH3"

/product="dual specificity phosphatase 5"

/note="Derived by automated computational

analysis using

gene prediction method: BestRefSeq."

/transcript id="NM_004419.4"

CDS join(216..594,4815..4963,9029..9248,12114..12520)

/gene="DUSP5"

1 ggcttctagg gCGgCGagCG gcCGggctgg ctatCGagCG agCGgggCGg
gaaCGCGgag

181 gCGgCGCGgg gcCGctggcc ggCGgCGgCG gCGgcatgaa ggtcaCGtCG
ctCGaCGggc

Homo sapiens chromosome 10, GRCh38.p13

Primary Assembly

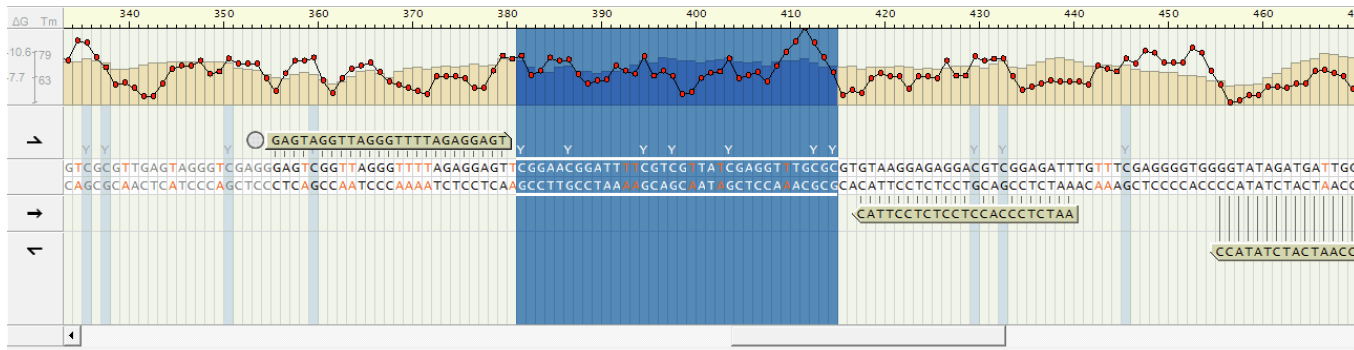
NCBI Reference Sequence: NC_000010.11

[GenBank Graphics](#)

>NC_000010.11:110495907-110511533 Homo sapiens chromosome 10,
GRCh38.p13 Primary Assembly

CCACTCTCAAATAAAGCACCGATCCCGCACAGAGCCGCTCAGCGATGTTCCCAAATGCTATCCG
GATCTTGTCACTGAGTAAGATCCCTCGTTGGGGACTGCCCGGCCAAAGACTAAGACCCAAATGACTCAA
AACAGCACAAGGCCCTCTGTTGCCTGACCCTGCTTAATCTGCTAATAAATACCAGAAGGGCCTTAGTCT
CCCACATACTCCAGTACCGCACCATGCTGGGGGGTTCGTTTTTTGTTTTCTTTACCCCAAGCAGTTT
CCTCTGCCTGGAATCTCCCTCCTGCTTCGACGCTGGCTTACAATTCATTCCTCGGAGTTGGCCTCAG
CTCTCCTCTCCTCGGGAGGCCCTTCTCCAGCCCACGCCCCACCCTGCCACACCCCTACTGGGCGCTCTTC
CCCACGGACTACAGGCCTTCCCTTCCCTCTGGGCTGGGGCAGCTGGGGCTGAGTATAAGTCTTACTC
ACGTTGGTGCCGCCAGCCCCAAAACAAAGCCTGGCCCACTGGGTGCTCCGCGTATGTGTGTGGCTCTA
GGCGGAGATGCCGGGGTGGAAAAGAGCGGTAACAGAAAAGAGAACTGCTAGAGGAAGAGCAGCCTGCA
GGGAAGGCTGGCACAGATAACCACAAAAAGAAAGAGGCCCGCATCACGCTTTCACCAAGACCCAC
TGGCAAGGCGAGGACAGCGCCTTTGGGTGGATGCATCTGTGACCCAGAGGCAATGCTGGCTGTCTGGT
GTCTGATTTGATTGCATCTGATTTCAAATTTGATCTCTGCTTCCCTTCTGAAAACCTCATTCCCTTATG
TCAGTTGTCAACAAGCCCTTGTCTAGTGGGCGAGACTGTTTTCCATCAAGCAGTCCCAGCCAGGCTAA
CAATAAAATGGTTGGCAGTGAAGCTTGGGGCAGAAAACCTGTTTCCATCCATGTGTCCCAGCAGCTAGCA
AAGCCCTGGCACACGCTGACCCCTCAATAAATGCTTGTGAATGGGTGAATGTGTCTGCTTCCCAGG
AATAGGGGTGGGAGGCCGTAAGCCCTGGGGACCGTGGGGGCAGACAGCCTGAGATTAACCTTGATCC
ATAGATAATCCCCAAATCCAGAAGCCACCTGGACAACAGTTGGCTGAAGTGAAGTCCATCGTGGGATA
CATGCTGATGGTACTGCTGAGTTCACCAAGGGTCTCCCAGGACCAGAAAACAGCTCCTCAAATACAA
CTTATTATTCTAATCATTATTGGAGAGTGACAGAGAAAAGAGCGTCAATCCTTTGAGGGCAGAATCCAT
TTAGGAAGATTAAATGGCTATTCTCACCGCGACCCCAACCCCGTTTTTACTTTTACAAACTTTATT
ATGAAAAATATCAAACATACAGAAAAAGTGGAGAAAAACAGTATAACGAATCGGCCACCCATCACCCAGC
CTCAGCGATGACCAACCAGCGCCTGACCTCTCCAGTCATCTATACCCACCCCTCGAGGCAAAATCTCCG
ACGTCCTCTCCTTACAACGCGCAGACCTCGGTAGCGACGGAATCCGTTCCGACTCCTCTGGGGCCCT
GGCAGGCTCCCTCGGCCCTGCTAGCGCGGGCGGGCGGGTTCTCAGCCCACTCGTCCGGAAGCTGAAG
GCCGCGATCGTGGCGCGCGCCCGCCCCCACTCGCGCTTCCCTCCTCGGTCCGACCGCGAGGGTACCG
CGGCCCGGAGCGCCTGGGACACTCGACCGGCAGCGCGGGTATGCGCGAGTGAGTCCCTCAGCGAAG
CGCGGAAGAGAGAAAGAAAGAGCGCCTTCCACTTCCCTCTCGCTCTAACCGCGCACCCCGCCCAGCGCGT
CCCTCGCCCCCGCTGCCCAGCCCCCTGCAGGGCGTGGCCAAGGCCGAGGGGCGGGAAACACCCATAT
TTGGCCTTATATGGGCAGCGCGTCAAGGACCGGCACTCATTCACATAAAAAGCTGCGCGGCCGCGGAA
TCCCAGGCTTCTAGGGCGCGAGCGGCAGGGCTGGCTATCGAGCGAGCGGGCGGGAAAGCGCGAGTTGC
GCCCGCTCGGGCGCGGGCTCCGTCGCGGCAGCGCGGGTCCCGTCCCTCGTGCCTCGCCCGC
GGACACCCTGGCCTGGACACCCTGGCCTGGGCACCAGCGGGGCGCGCGCGCGGGGCGCTGGCCCG
CGCGCGCGCGGCATGAAGGTCACTCGCTCGACGCGGGCCAGCTGCGCAAGATGCTCGCAAGGAGGC
GGCGCGCGCTCGTGGTGCTCGACTGCGGCCCTATCTGGCCTTCTCGTGCCTCGAACGTCGCGGCTC
GCTCAACGTC AACCTCAACTCGGTGGTGCTGCGCGGGCCCGGGCGCGCGGTGTGCGCGCGCTACGT
GCTGCCCGAAGGCGCGCGCGCGCGCTCCTGCAGGAGGGCGCGCGCGCGTCCGCGCGTGGTGGT
GCTGGACCAGGGCAGCGCCACTGGCAGAAGCTCGAGAGGA

Inverse complement sequence design:



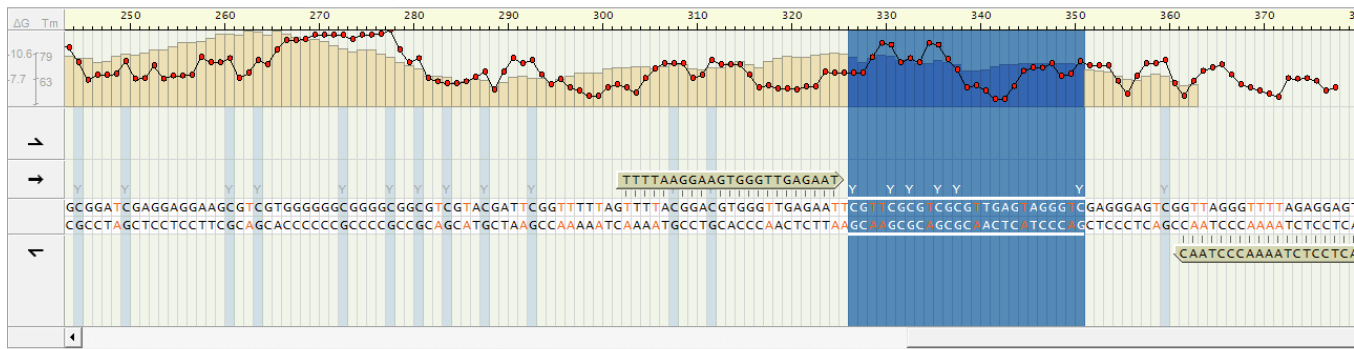
Primer Set 1	Score: 89
General Warnings	

F1	GAGTAGGTTAGGGTTTTAGAGGAGT
R1	AACCTCTCCAATCATCTATACC
S1	AATCTCCACCTCCTCTCCTTAC

Primer Set 1	Score: 89
General Warnings	

F1	GAGTAGGTTAGGGTTTTAGAGGAGT
R1	AACCTCTCCAATCATCTATACC
S1	AATCTCCACCTCCTCTCCTTAC

	PCR Product	Forward PCR Primer, F1	Reverse PCR Primer, R1	Sequencing Primer, S1
Length, nt	122	25	22	23
Position, 5'- 3'		355 - 379	476 - 455	439 - 417
Warnings				
Tm, °C		59.9	57.9	44.3
%GC	41.0	44.0	40.9	52.2
Sequence to Analyze	ACRCRCAAAC CTRATAACR ACRAAAATCC RTTCRAACT CCTCTAAAC CCTAAC			



Primer Set 1	Score: 76
General Warnings	

F1	TAGAGAGAGGAAGTGAAGG
R1	AACCTCTTAAACCTAAC
S1	TTTTAAGGAAGTGGGTTGAGAAT

Primer Set 1	Score: 76
General Warnings	

F1	TAGAGAGAGGAAGTGAAGG
R1	AACCTCTTAAACCTAAC
S1	TTTTAAGGAAGTGGGTTGAGAAT

	PCR Product	Forward PCR Primer, F1	Reverse PCR Primer, R1	Sequencing Primer, S1
Length, nt	269	22	20	23
Position, 5'- 3'		112 - 133	380 - 361	302 - 324

Warnings	Deviation from optimal amplicon size			
Tm, °C		57.5	55.8	44.1
%GC	39.4	50.0	40.0	34.8
Sequence to Analyze	TYGTTYGYGT YGYGTTGAGT AGGGTYGAGG GAGTYGGTTA GGGTTTTAGA G			

[Supplemental table 6 and Supplemental table 7: The mRNA variation abundance for TUG1-knockdown in HTR-8/SVneo cells, which can be found online at Xu et al^{\[1\]}](#)

[1]Xu, Y., Ge, Z., Zhang, E., Zuo, Q., Huang, S., Yang, N., Wu, D., Zhang, Y., Chen, Y., Xu, H., Huang, H., et al. (2017). The lncRNA TUG1 modulates proliferation in trophoblast cells via epigenetic suppression of RND3. *Cell Death Dis* 8, e3104. 10.1038/cddis.2017.503.